Inorganic Chemistry
Article

Inorg. Chem. **2011**, *50*, 503–516 **503**
DOI: 10.1021/ic101587h

Binding of a Coordinatively Unsaturated Mercury(II) Thiolate Compound by Carboxylate Anions

Xiao-Yan Tang,[†,‡,§] Ai-Xia Zheng,[†] Hai Shang,[†] Rong-Xin Yuan,[§] Hong-Xi Li,[†] Zhi-Gang Ren, and Jian-Ping Lang*[,†,‡]

[†]*College of Chemistry, Chemical Engineering and Materials Science, Soochow University, Suzhou 215123, People's Republic of China,* [‡]*State Key Laboratory of Coordination Chemistry, Nanjing University, Nanjing 210093, People's Republic of China, and* [§]*Jiangsu Laboratory of Advanced Functional Materials, Changshu Institute of Technology, Changshu 215500, People's Republic of China*

Received August 5, 2010

Reactions of $[Hg(Tab)_2](PF_6)_2$ (TabH = 4-(trimethylammonio)benzenethiol) (**1**) with acetic acid (HAc), propanoic acid (HPro), salicylic acid (HSal), benzoic acid (HBez), malonic acid (H_2Mal), oxalic acid (H_2Oxa), adipic acid (H_2Adi), or methylimindiacetic acid (H_2Meida) in the presence of Et_3N gave rise to a family of mercury(II)-thiolate-carboxylate compounds, $[Hg(Tab)_2(Ac)](PF_6)\cdot 0.5H_2O$ (**2**$\cdot 0.5H_2O$), $[Hg(Tab)_2(Pro)](PF_6)$ (**3**), $[Hg(Tab)_2(Sal)](PF_6)\cdot MeOH$ (**4**$\cdot$MeOH), $[Hg(Tab)_2(Sal)](Sal)\cdot MeOH$ (**5**$\cdot$MeOH), $[Hg(Tab)_2(Bez)](PF_6)\cdot H_2O$ (**6**$\cdot H_2O$), $[Hg(Tab)_2(HMal)]$-$(Mal)_{0.5}\,H_2O$ (**7**$\cdot H_2O$), $[\{Hg(Tab)_2\}_2(\mu\text{-Oxa})](PF_6)_2\,H_2O$ (**8**$\cdot 2H_2O$), $[\{Hg(Tab)_2\}_2(\mu\text{-Adi})](PF_6)_2$ (**9**), $[Hg(\mu\text{-Tab})$-$(\mu\text{-Adi})]_{2n}$ (**10**), and $[Hg(Tab)_2(Meida)]\cdot 2.5H_2O$ (**11**$\cdot 2.5H_2O$). These compounds were characterized by elemental analysis, IR spectra, UV−vis spectra, ^{1}H NMR, and single-crystal X-ray crystallography. Each mercury(II) atom in $[Hg(Tab)_2]^{2+}$ dication of **2**−**7** is further coordinated by two oxygen atoms from one Ac^-, Pro^-, Sal^-, Bez^-, Mal^{2-} or $HMal^-$ anion, forming a unique seesaw-shaped coordination geometry. In **8** or **9**, two $[Hg(Tab)_2]^{2+}$ dications are connected by one bridging oxalate or adipate dianion to generate a dimeric structure with each mercury(II) center adopting a seesaw-shaped geometry. In **10**, a pair of octahedrally coordinated mercury(II) atoms are bridged by two sulfur atoms of two Tab ligands to form a $[Hg(\mu\text{-Tab})_2Hg]^{4+}$ fragment, which is further connected to its equivalent ones via four adipate dianions, thereby forming a rare two-dimensional network. In **11**, the mercury(II) atom in the $[Hg(Tab)_2]^{2+}$ dication is coordinated by one nitrogen and two oxygen atoms from one $Meida^{2-}$ dianion to have a rare square pyramidal geometry. The formation of **2**−**11** from **1** may be applicable to mimicking the interactions of the mercury(II) sites of Hg-MerR and Hg-MT with various amino acids encountered in nature.

Introduction

In our previous studies, we reported the preparation of the mononuclear mercury(II) complex $[Hg(Tab)_2](PF_6)_2$ (TabH = 4-(trimethylammonio)benzenethiol) (**1**) using a zwitterionic thiol $TabHPF_6$.[1a] Complex **1** was employed as a potential model complex for mimicking the reactivity of unsaturated HgS_2 sites in the detoxification of mercury by metallothioneins (MTs),[2] in DNA binding-proteins,[3] and in the mercury reductase and organomercury lyase,[4] and metalloregulatory protein (MerR).[5] The reactions of **1** with some donor ligands (e.g., Tab, NCS^-, I^-), the naturally encountered inorganic anions (e.g., Cl^-, NO_2^-, NO_3^-), organic amines and nitrogen heterocyclic compounds (e.g., 1,2-diaminoethane, pyridine, 1,10-phenanthroline, *N*-methylimidazole) were investigated.[1] In most of these reactions, the unsaturated coordination geometry of the mercury(II) center in **1**, involving a linear S−Hg−S unit with

*To whom correspondence should be addressed. E-mail: jplang@suda.edu.cn.

(1) (a) Chen, J. X.; Zhang, W. H.; Tang, X. Y.; Ren, Z. G.; Zhang, Y.; Lang, J. P. *Inorg. Chem.* **2006**, *45*, 2568. (b) Chen, J. X.; Xu, Q. F.; Xu, Y.; Zhang, Y.; Chen, Z. N.; Lang, J. P. *Eur. J. Inorg. Chem.* **2004**, 4247. (c) Chen, J. X.; Xu, Q. F.; Zhang, Y.; Chen, Z. N.; Lang, J. P. *J. Organomet. Chem.* **2004**, *689*, 1071. (d) Chen, J. X.; Zhang, W. H.; Tang, X. Y.; Ren, Z. G.; Li, H. X.; Zhang, Y.; Lang, J. P. *Inorg. Chem.* **2006**, *45*, 7671. (e) Ren, Z. G.; Tang, X. Y.; Li, L.; Liu, G. F.; Li, H. X.; Chen, Y.; Zhang, Y.; Lang, J. P. *Inorg. Chem. Commun.* **2007**, *10*, 1253. (f) Tang, X. Y.; Chen, J. X.; Liu, G. F.; Ren, Z. G.; Zhang, Y.; Lang, J. P. *Eur. J. Inorg. Chem.* **2008**, 2593. (g) Tang, X. Y.; Li, H. X.; Chen, J. X.; Ren, Z. G.; Lang, J. P. *Coord. Chem. Rev.* **2008**, *252*, 2026. (h) Tang, X. Y.; Yuan, R. X.; Ren, Z. G.; Li, H. X.; Zhang, Y.; Lang, J. P. *Inorg. Chem.* **2009**, *48*, 2639.

(2) (a) Stillman, M. J.; Law, A. Y. C.; Szymanska, J. A. In *Chemical Toxicology and Clinical Chemistry of Metals*; Brown, S. S., Savoy, J., Eds.; Academic: London, 1983; p 275. (b) Cheesman, B. V.; Arnold, A. P.; Rabenstein, D. Z. *J. Am. Chem. Soc.* **1988**, *110*, 6359. (c) Nielsen, K. B.; Atkin, C. L.; Winge, D. R. *J. Biol. Chem.* **1985**, *260*, 5342. (d) Wright, J. G.; Natan, M. J.; MacDonnell, F. M.; Ralston, D. M.; O'Halloran, T. V. *Prog. Inorg. Chem.* **1990**, *38*, 323. (e) Sigel, A.; Sigel, H. *Metal Ions in Biological Chemical Toxicology and Clinical Chemistry of Metals*; Brown, S. S., Savoy, J., Eds.; Dekker: New York, 1997. (f) Fleischer, H.; Dienes, Y.; Mathiasch, B.; Schmitt, V.; Schollmeyer, D. *Inorg. Chem.* **2005**, *44*, 8087. (g) Lippard, S. J.; Berg. J. M. *Principles of Bioinorganic Chemisty*; University Science: Mill Valley, CA, 1994. (h) Baba, K.; Okamura, T.; Yamamoto, H.; Yamamoto, T.; Ueyama, N. *Inorg. Chem.* **2008**, *47*, 2837. (i) Vig, K.; Megharaj, M.; Sethunathan, N.; Naidu, R. *Adv. Environ. Res.* **2003**, *8*, 121.

(3) (a) Kuklenyik, Z.; Marzilli, L. G. *Inorg. Chem.* **1996**, *35*, 5654. (b) Utschig, L. M.; Wright, J. G.; O'Halloran, T. *Methods Enzymol.* **1993**, *226*, 71. (c) Patra, G. K.; Goldberg, I. *Polyhedron* **2002**, *21*, 2195. (d) Dance, I. G. *Polyhedron* **1986**, *5*, 1037. (e) Henkel, G.; Krebs, B. *Chem. Rev.* **2004**, *104*, 801. (f) Engst, S.; Miller, S. M. *Biochemistry* **1999**, *38*, 3519.

Published on Web 12/14/2010

strong bonding to sulfur atoms, was further completed by additional donor ligands. The sulfur atoms of Tab ligands in **1** were also witnessed to further bind to additional metal atoms. In a rare case, one of the Hg−S(Tab) bonds in **1** was broken up and the rest mercury(II)/Tab species were rearranged into different mercury(II)/Tab compounds.[1a] Considering that organic carboxylic acids are always encountered in nature, can they, like those inorganic anions and organic amines, react with **1** and change the geometry of the mercury(II) center in **1**?

Reactions of organic or inorganic mercury(II) compounds with various carboxylic acids and amino acids have been well documented and some mercury compounds containing acetate,[6] nicotinate,[7] α-picolinate,[8] pyridine-2,6-dicarboxylate,[9] pyridyl-acetate,[10] 2-amino-4-phenylbutyrate,[11] 2-pyrazinecarboxylate,[12] 2,6-diamino-hexanoate,[13] cysteine,[14] homocysteine,[15] *S*-methyl-cysteine,[16] methionine,[16a,17] penicillamine,[17a,18] proline,[19] serine,[20] alanine,[21] tryptophan,[15] *N*-acetyl-DL-tryptophan,[22] and dipeptide glycylglycine[23] have been structurally characterized. However, the interactions between the carboxylic acids and the mercury(II)/thiolate compounds, especially those containing the unsaturated HgS_2 site, seem almost unexplored. In this article, we deliberately selected two alkyl carboxylic acids [acetic acid (HAc) and propanoic acid (HPro)], two aryl acids [salicylic acid (HSal) and benzoic acid (HBez)], three dicarboxylic acids [malonic acid (H_2Mal), oxalic acid (H_2Oxa), adipic acid (H_2Adi)], and one amino acid [methylimindiacetic acid (H_2Meida)] to react with **1** in the presence of Et_3N, and a set of mercury(II)-thiolate-carboxylate compounds (**2**−**11**) were isolated and characterized. Herein we report the reactions of **1** with these carboxylic acids and their isolation and spectral and structural characterization.

Results and Discussion

Synthetic and Spectral Aspects. Reactions of **1** and various carboxylic acids are relatively straightforward. Treatment of **1** with a slight excess acetate acid or propionic acid in MeOH/H_2O under the presence of Et_3N gave rise to the mononuclear compound $[Hg(Tab)_2(Ac)](PF_6)\cdot 0.5H_2O$ (**2**$\cdot 0.5H_2O$) or $[Hg(Tab)_2(Pro)](PF_6)$ (**3**) as colorless blocks in 77% yield (**2**$\cdot 0.5H_2O$) or 92% yield (**3**) (Scheme 1). When **1** reacted with 1 or 2 equiv of salicylic acid, it afforded the expected compounds $[Hg(Tab)_2(Sal)](PF_6)\cdot$MeOH (**4**$\cdot$MeOH) or $[Hg(Tab)_2(Sal)](Sal)\cdot$MeOH (**5**$\cdot$MeOH) as long needles in 87% yield (**4**$\cdot$MeOH) or 78% yield (**5**$\cdot$MeOH). The similar reactions of **1** with benzoic acid in 1: 1 or 1: 2 molar ratio only generated $[Hg(Tab)_2(Bez)](PF_6)\cdot H_2O$ (**6**$\cdot H_2O$) in 86% yield.

In addition, several carboxylic diacid ligands were also introduced into the mercury/thiolate system and several Hg/Tab/polycarboxylate compounds were isolated. For instance, the reaction of **1** with malonic acid in the presence of Et_3N did not produce the expected dimeric compound $\{[Hg(Tab)_2]_2(\mu\text{-Mal})\}(PF_6)_2$, but formed a mononuclear compound $[Hg(Tab)_2(HMal)](Mal)_{0.5}\cdot H_2O$ (**7**$\cdot H_2O$) as colorless blocks in 82% yield (Scheme 2). An analogous reaction of **1** with oxalic acid afforded a dimeric compound $[\{Hg(Tab)_2\}_2(\mu\text{-Oxa})](PF_6)_2\cdot 2H_2O$ (**8**$\cdot 2H_2O$) in 89% yield. Intriguingly, the reaction of **1** with equimolar adipic acid in MeOH led to the formation of an expected dimeric compound $[\{Hg(Tab)_2\}_2(\mu\text{-Adi})](PF_6)_2$ (**9**) in 81% yield (Scheme 3). However, the similar reaction with same components in a ratio of 1:2 gave rise to a rare polymeric compound $[Hg(\mu\text{-Tab})(\mu\text{-Adi})]_{2n}$ (**10**). In this reaction, one Tab ligand in $[Hg(Tab)_2]^{2+}$ of **1** was replaced by the adipate dianion while each mercury(II) center is coordinated by two doubly bridging Tab ligands and four doubly bridging adi dianions as described later in this article. The formation of **10** might be ascribed to its low solubility in MeCN.

Finally, treatment of **1** with methylimindiacetic acid followed by a standard workup afforded the neutral compound $[Hg(Tab)_2(Meida)]_2\cdot 2.5H_2O$ (**11**$\cdot 2.5H_2O$) (Scheme 4), in which one N and two O atoms of Meida bind to the center mercury atom. It is noted that in the

(4) (a) Blower, P. J.; Dilworth, J. R. *Coord. Chem. Rev.* **1987**, *76*, 121. (b) Bharara, M. S.; Parkin, S.; Atwood, D. A. *Inorg. Chem.* **2006**, *45*, 7261. (c) Bharara, M. S.; Bui, T. H.; Parkin, S.; Atwood, D. A. *J. Chem. Soc., Dalton Trans.* **2005**, 3874. (d) Wright, J. G., Natan, M. J., MacDonnell, F. M., Ralston, D. M., O'Halloran, T. V. *Mercury(II)-Thiolate Chemistry and the Mechanism of the Heavy Metal Biosensor MerR*; John Wiley & Sons: New York, 1990. (e) Stillman, M. J.; Shaw, C. F.; Suzuki, K. T. *Metallothioneins: Synthesis, Structure and Properties of Metallothioneins, Phytochelatins and Metal-Thiolate Complexes*; John Wiley & Son: New York, 1992. (f) Chan, J.; Huang, Z. Y.; Merrifield, M. E.; Salgado, M. T.; Stillman, M. J. *Coord. Chem. Rev.* **2002**, *233*−*234*, 319. (g) Qian, H.; Sahlman, L.; Eriksson, P. O.; Hambraeus, C.; Edlund, U.; Sethson, I. *Biochemistry* **1998**, *37*, 9316.

(5) (a) Moore, M. J.; Distefano, M. D.; Zydowsky, L. D.; Cummings, R. T.; Walsh, C. T. *Acc. Chem. Res.* **1990**, *23*, 301. (b) Ralston, D. M.; O'Halloran, T. V. *Adv. Inorg. Biochem.* **1990**, *8*, 1. (c) Gruff, E. S.; Koch, S. A. *J. Am. Chem. Soc.* **1990**, *112*, 1245. (d) Helmann, J. D.; Shewchuk, L. M.; Walsh, C. T. *Adv. Inorg. Biochem.* **1990**, *8*, 33. (e) Govindaswamy, N.; Moy, J.; Millar, M.; Koch, S. A. *Inorg. Chem.* **1992**, *31*, 5343. (f) Adams, M. J.; Hodgkin, D. C.; Raeburn, U. A. *J. Chem. Soc. A* **1970**, 2632.

(6) Grdenic, D.; Sikirica, M.; Korpar-Colig, B. *Croat. Chem. Acta* **1989**, *62*, 27.

(7) Popovic, Z.; Pavlovic, G.; Matkovic-Calogovic, D.; Soldin, Z. *Acta Crystallogr., Sect. C* **2003**, *59*, m165.

(8) (a) Popovic, Z.; Pavlovic, G.; Soldin, Z. *Acta Crystallogr., Sect. C* **2006**, *62*, m272. (b) Alvarez-Larena, A.; Piniella, J. F.; Pons, J.; March, R.; Casabo, J. *Z. Kristallogr.* **1994**, *209*, 695.

(9) (a) Aghabozorg, H.; Ghasemikhah, P.; Ghadermazi, M.; Gharamaleki, J. A.; Sheshmani, S. *Acta Crystallogr., Sect. E* **2006**, *62*, m2269. (b) Moghimi, A.; Shokrollahi, A.; Shamsipur, M.; Aghabozorg, H.; Ranjbar, M. *J. Mol. Struct.* **2004**, *701*, 49. (c) Bao, T. H.; Hou, Z. Y. *Acta Crystallogr., Sect. E* **2006**, *62*, m801. (d) Matkovic-Calogvic, D.; Popovic, J.; Popovic, Z.; Picek, I.; Soldin, Z. *Acta Crystallogr., Sect. C* **2002**, *58*, m39. (e) Aghabozorg, H.; Bagheri, S.; Heidari, M.; Ghadermazi, M.; Gharamaleki, J. A. *Acta Crystallogr., Sect. E* **2008**, *64*, m1065.

(10) Du, M.; Li, C. P.; Zhao, X. J. *Cryst. Growth Des.* **2006**, *6*, 335.

(11) Alcock, N. W.; Lampe, P. A.; Moore, P. *J. Chem. Soc., Dalton Trans.* **1978**, 1324.

(12) Dong, Y. B.; Smith, M. D.; Loye, H. C. *Angew. Chem., Int. Ed.* **2000**, *39*, 4271.

(13) Zabel, M.; Poznyak., A. L.; Pavloskii, V. I. *Zh. Neorg. Khim.* **2005**, *50*, 1991.

(14) (a) Taylor, N. J.; Wong, Y. S.; Chieh, P. C.; Carty, A. J. *J. Chem. Soc., Dalton Trans.* **1975**, 438. (b) Taylor, N. J.; Carty, A. J. *J. Am. Chem. Soc.* **1977**, *99*, 6143.

(15) Book, L.; Carty, A. J.; Chieh, C. *Can. J. Chem.* **1981**, *59*, 138.

(16) (a) Wong, Y. S.; Taylor, N. J.; Chieh, P. C.; Carty, A. J. *J. Chem. Soc., Chem. Commun.* **1974**, 625. (b) Book, L.; Carty, A. J.; Chieh, C. *Can. J. Chem.* **1981**, *59*, 144.

(17) (a) Carty, A. J.; Taylor, N. J. *J. Chem. Soc., Chem. Commun.* **1976**, 214b. (b) Wong, Y. S.; Carty, A. J.; Chieh, P. C. *J. Chem. Soc., Dalton Trans.* **1977**, 1157.

(18) (a) Wong, Y. S.; Chieh, P. C.; Carty, A. J. *Can. J. Chem.* **1973**, *51*, 2597. (b) Wong, Y. S.; Carty, A. J.; Chieh, P. C. *J. Chem. Soc., Dalton Trans.* **1977**, 1801. (c) Book, L.; Mak, T. C. W. *Inorg. Chim. Acta* **1984**, *92*, 265.

(19) (a) Ehsan, M. Q.; Malik, K. M. A.; Haider, S. Z. *J. Bangladesh Acad. Sci.* **1996**, *20*, 175. (b) Kalaiselvi, D.; Kumar, R. M.; Jayavel, R. *Acta Crystallogr., Sect. E* **2008**, *64*, m1048.

(20) Corbeil, M. C.; Beauchamp, A. L. *Can. J. Chem.* **1988**, *66*, 1379.

(21) (a) Corbeil, M. C.; Beauchamp, A. L. *Can. J. Chem.* **1986**, *64*, 1876. (b) Corbeil, M. C.; Beauchamp, A. L. *J. Crystallogr. Spectrosc. Res.* **1989**, *19*, 123. (c) Saunders, C. D. L.; Burdord, N.; Werner-Zwanziger, U.; McDonald, R. *Inorg. Chem.* **2008**, *47*, 3693.

(22) Corbeil, M. C.; Beauchamp, A. L. *Can. J. Chem.* **1988**, *66*, 2458.

(23) Corbeil, M. C.; Beauchamp, A. L. *Can. J. Chem.* **1986**, *64*, 148.

Scheme 1. Reactions of **1** with Acetic Acid, Propionic Acid, Salicylic acid, and Benzoic acid in the Presence of Et_3N

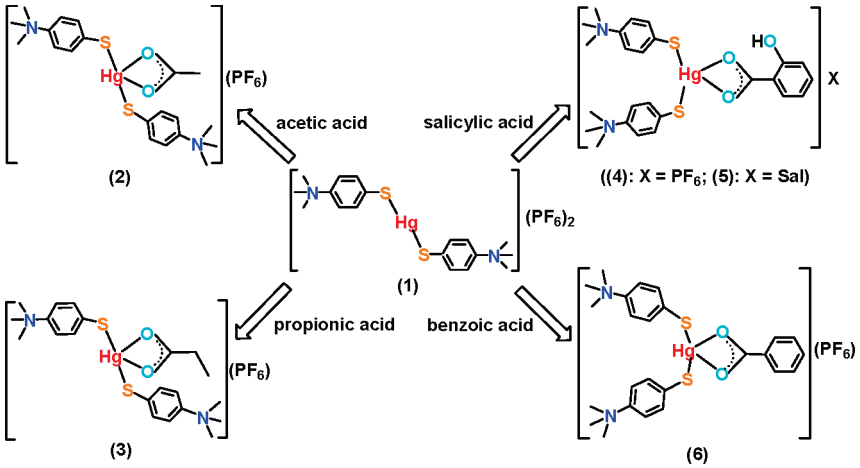

Scheme 2. Reactions of **1** with Malonic Acid and Oxalic Acid in the Presence of Et_3N

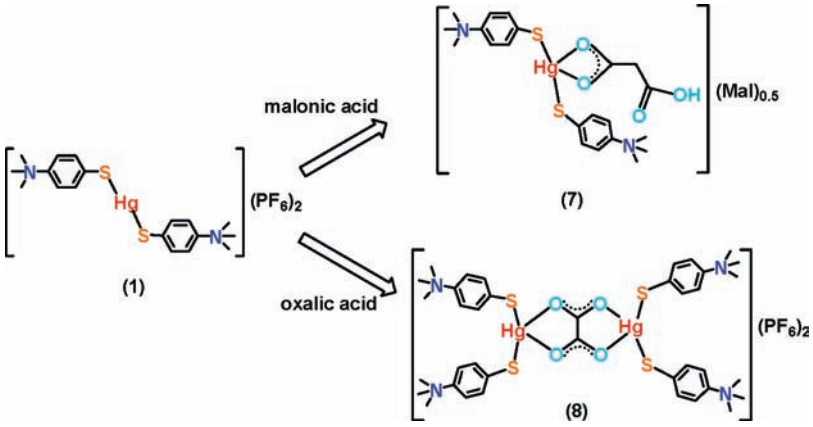

Scheme 3. Reactions of **1** with 1 or 2 Equivalents of Adipic Acid in the Presence of Et_3N

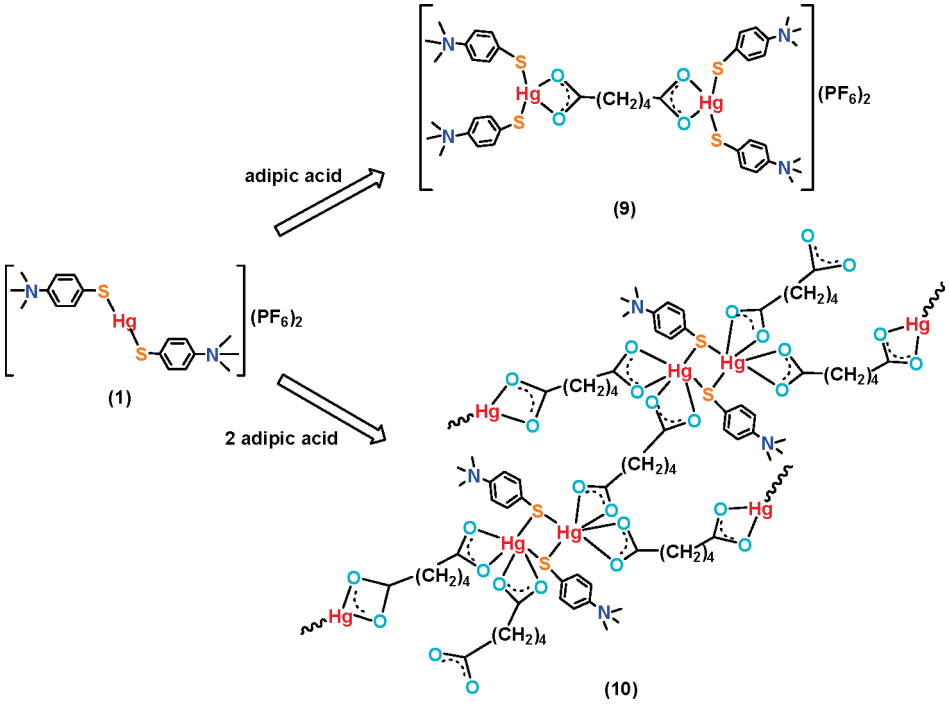

Scheme 4. Reactions of **1** with Methylimidizole Diacid in the Presence of Et_3N

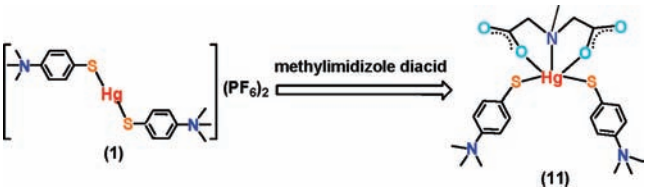

formation of **2**−**11**, the carboxylic acid was deprotonated by Et_3N, thereby forming a protonated $[Et_3NH]^+$ cation. Part of the resulting carboxylate anion in **5** and **7** worked as a counteranion for the resulting $[Hg(Tab)_2L]^+$ (L = Sal^-, Mal^{2-}) cation. The eliminated $[PF_6]^-$ anion may combine $[Et_3NH]^+$ to form $[Et_3NH]PF_6$, which may remain in solution during the crystallization.

Compounds **2**−**11** were stable toward oxygen and moisture, and readily soluble in dimethylsulfoxide (DMSO), dimethylformamide (DMF), MeCN, and insoluble in MeOH, EtOH, CH_2Cl_2, and benzene. The elemental analyses were consistent with their chemical formula. Compound **2**, **3**, or **11** exhibits ν_a(COO) and ν_s(COO) of the related carboxylate anion at 1552 (**2**), 1547 (**3**), or 1589 (**11**) and 1490 (**2**), 1491 (**3**), or 1489 (**11**) cm^{-1}, respectively.[24] In the IR spectra of **4**−**6**, the bands at 1558/1488 cm^{-1} (**4**), 1585/1488 cm^{-1} (**5**), or 1548/1489 cm^{-1} (**6**) can be assigned to be the symmetric and asymmetric C−O stretching vibrations of salicylate or benzolate ligand. In the case of **7**, the presence of the characteristic band at 1732 cm^{-1} indicates that the deprotonation of malonic acid is incomplete, though it shows ν(C═O) at 1621 and 1489 cm^{-1}. In the IR spectra of **8**−**10**, a strong band at 1655 (**8**), 1630 (**9**), or 1638 (**10**) cm^{-1} may be assigned to be the C−O stretching vibration for a tetradentate bridging oxalate or adipate. In the IR spectra of **2**−**4**, **6**, **7**, and **9**, bands at about 838 and 558 cm^{-1} may be assignable to the characteristic P−F stretching vibrations of PF_6^-. The absorption peaks at 3400−3500 cm^{-1} are assigned to ν(OH) of the uncoordinated water molecules. In the ^{1}H NMR spectra of **2**−**7** and **9**−**11** in DMSO-d_6 at ambient temperature, resonances related to the protons of the carboxylate anions are assigned as follows: a singlet at 1.69 ppm for methyl protons of acetate (**2**), multiplets at 1.88−1.93 ppm and 0.89−0.93 ppm for methylene and methyl protons of propionate (**3**), multiplets at 7.62−7.65 ppm, 7.09−7.15 ppm, 6.55−6.62 ppm (**4** and **5**), and a broad singlet at 4.05 ppm (**4**) or 4.08 ppm (**5**) for phenyl and hydroxyl protons of Sal ligand (**4** and **5**), multiplets at 7.80−7.82 ppm and 7.29−7.37 ppm for phenyl protons of benzoate (**6**), multiplets at 2.97−2.99 ppm (**7**), 1.94 ppm and 1.43 ppm (**9**), 1.90 ppm and 1.50−1.52 ppm (**10**) for methylene protons of Mal or Adi ligands, singlet at 2.16 ppm and multiplets at 2.94 ppm for methyl and methylene protons of Meida ligand (**11**). It is noted that resonances related to the protons of the Tab ligand in **2**−**11** feature multiplets in the region of 7.51−7.72 ppm for its phenyl groups of the Tab ligands and a singlet at about 3.53 ppm for the methyl protons of its NMe_3 unit. These peaks exhibited some shifts from those of the corresponding ones of the free ligand Tab [δ 7.36−7.53 (m, 4H, Ph), 3.36 (9H, m, NMe_3)], but did not show much shifting from those of the corresponding ones of **1**.[1a] The results suggest that binding of the carboxylate anions to the mercury(II) centers of **2**−**11** in DMSO-d_6 solution may be weak.

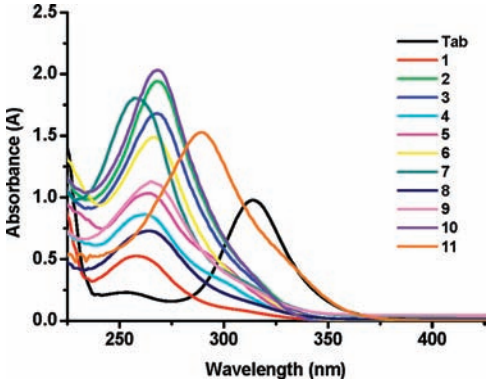

Figure 1. UV−vis curves for the acetonitrile solutions of 1.0×10^{-5} M for **1**, 2.0×10^{-5} M for **2**, 2.0×10^{-5} M for **3**, 1.0×10^{-5} M for **4**, 1.0×10^{-5} M for **5**, 1.0×10^{-5} M for **6**, 1.0×10^{-5} M for **7**, 2.0×10^{-5} M for **8**, 1.0×10^{-5} M for **9**, 2.0×10^{-5} M for **10**, 2.0×10^{-5} M for **11**, and 1.0×10^{-5} M for Tab.

As shown in Figure 1, the electronic spectra of **2**−**11** in MeCN exhibit a strong and broad absorption with maxima values ranging from 258 to 290 nm and a long absorption tail to about 400 nm. Those main absorption bands observed in the spectra of **2**−**11** are blue-shifted with respect to the absorption band at 314 nm of the Tab ligand,[1a] which may be ascribed to the ligand(Tab)-to-metal charge transfer (LMCT).[25] When additional carboxylate anions are introduced into the $[Hg(Tab)_2]^{2+}$ linear framework of **1**, the main absorptions observed in the spectra of **2**−**10** look similar and are slightly blue-shifted relative to that of **1**, which may reflect that the mercury(II) atoms in **2**−**10** adopt a different coordination environment. Currently it is difficult to clearly and accurately correlate the UV−vis absorption data (the position and/or intensity of the bands), for example, with structural features like Hg−S bond lengths, S−Hg−S angles, or other structural properties. However, we could still find some interesting correlations through comparison with those of the existing mercury(II) thiolate compounds (Table 1). As observed in Hg(II)-MerR/MT, $[Hg(SR)_2]$ (R = Et and ^{i}Pr),[26] mercury plastocyanin,[26d] and other metallothioneins,[27] the low-energy UV transitions of 228−250 nm may reflect the two- and three-coordination environments, while those at the range of 280−310 nm may represent a four-coordination geometry. The main absorptions in **2**−**10** are in the range of 258−268 nm, suggesting that the coordination geometry around the Hg atom in these compounds may not be trigonally or tetrahedrally coordinated but in-between three and

(24) Nakamoto, K. *Infrared and Raman Spectra of Inorganic and Coordination compounds*, Part B: Applications in Coordination, Organometallic, and Bioinorganic Chemistry, 5th ed.; John Wiley & Sons, Inc.: New York, 1997.

(25) (a) Schaffer, A.; Williman, K.; Willner, H. *J. Inorg. Biochem.* **1989**, *36*, 186. (b) Bharara, M. S.; Bui, T. H.; Parkin, S.; Atwood, D. A. *Inorg. Chem.* **2005**, *44*, 5753. (c) Bharara, M. S.; Parkin, S.; Atwood, D. A. *Inorg. Chem.* **2006**, *45*, 2112.

(26) (a) Watton, S. P.; Wright, J. G.; MacDonnell, F. M.; Bryson, J. W.; Sabat, M.; O'Halloran, T. V. *J. Am. Chem. Soc.* **1990**, *112*, 2824. (b) Vasak, M.; Kaegi, J. H. R.; Hill, H. A. O. *Biochemistry* **1981**, *20*, 2852. (c) Johnson, B. A.; Armitage, I. M. *Inorg. Chem.* **1987**, *26*, 3139. (d) Tamilarasan, R.; McMillin, D. R. *Inorg. Chem.* **1986**, *25*, 2037. (e) Schicht, O.; Eva Freisinger, E. *Inorg. Chim. Acta* **2009**, *362*, 714.

(27) Beltramine, M.; Lerch, K.; Vasak, M. *Biochemistry* **1984**, *23*, 3422.

Table 1. Principal Electronic Transitions in **1**−**11**, Tab, and Other Mercury(II) Thiolate Compounds

compound	λ_{max}, nm	ref.
[Hg(L-Cys)$_4$peptide][a]	280	25a
[$Hg_6Cl_8(SCH_2CH_2NH_3)_8$]] $Cl_4 \cdot 4H_2O$	273	25b
[$Hg_9Br_{15}(SCH_2CH_2NH_3)_9$]-$(Cl_{0.8}Br_{0.2})_3$	268, 339 (sh)[b]	25b
[$Hg(SEt)_2$]	228, 282 (sh)	26a
[$Hg(SPr^i)_2$]	228, 262 (sh)	26a
[Et_4N][$Hg(SBu^t)_3$]	235, 260 (sh)	26a
Hg-MerR[c]	240, 260 (sh), 290 (sh)	26a
Hg_7-MT[d]	304	26b, 26c
Hg-plastocynanin	247, 280 (sh)	26d
Hg-MT1[e]	253	26e
Neurospora Hg_3-MT	283	27
Tab	320, 267 (sh)	1a
[$Hg_2(Tab)_6$]$(PF_6)_4$	287, 312 (sh)	1a
[$Hg(Tab)_2(SCN)_2$]	271	1a
[$Hg(Tab)_2$(phen)]$(PF_6)_2$[f]	263	1h
[$Hg(Tab)_2$(2,2′-bipy)]$(PF_6)_2$[g]	258	1h
[$Hg(Tab)_2$(dap)]$(PF_6)_2$[h]	264	1h
[$Hg(Tab)_2$(dpt)]$(PF_6)_2$[i]	257	1h
1	272	1a
2	268	this work
3	267	this work
4	261	this work
5	264	this work
6	267	this work
7	258	this work
8	264	this work
9	265	this work
10	268	this work
11	290	this work

[a] L-Cys = L-cysteine. [b] sh = shoulder. [c] MerR = metalloregulatory protein. [d] MT = metallothionein. [e] MT1 = *Cicer arietinum* (chickpea) MT1. [f] phen = phenanthroline. [g] 2,2′-bipy = 2,2′-bipyridine. [h] dap = 1,3-diaminopropane. [i] dpt = dipropylenetriamine.

four-coordinated. These absorptions are similar to those of the mercury(II)/Tab/amine compounds reported previously, [$Hg(Tab)_2(L)$]$(PF_6)_2$ (L = phenanthroline, 2,2′-bipyridine, 1,3-diaminopropane, dipropylenetriamine).[1h] As described later in this article, each mercury(II) center in **2**−**9** adopts a similar seesaw-shaped coordination geometry to that found in the aforementioned mercury(II)/Tab/amine compounds, though that of **10** takes a distorted octahedral geometry. Compared to other mercury(II)/Tab/carboxylate compounds, the absorption peak in **11** (290 nm), red-shifted relative to that of **1**, may indicate existence of a different coordination geometry of the mercury(II) center coordinated by a different set of donor atoms. It is noted that compounds **9** and **10** contain the same set of ligands but different structures (as shown by the X-ray crystallographic studies), but their spectral data are quite similar. Is **10** stable in solution or is it converted to **9**? We measured the positive electrospray ion (ESI) mass spectra of **9** and **10** in MeCN. In both cases we did not observe the expected [$\{Hg(Tab)_2\}_2(\mu$-Adi)]$^{2+}$ peak. However, we obtained the same peak at m/z 268.06 corresponding to the [$Hg(Tab)_2$]$^{2+}$ cation (see Supporting Information, Figure S5). This result suggests that the adipate anions in **9** and **10** may not strongly coordinate to the mercury(II) centers and be readily cleaved in polar solvents like MeCN, which may lead to similar spectral data for both compounds in solution.

Crystal Structures of 2·0.5H_2O, 3, 4·MeOH, 5·MeOH, 6·H_2O, and 7·H_2O. X-ray analysis revealed that compounds **2**−**7** possess a similar structure that consists of one [$Hg(Tab)_2L$]$^+$ (L = Ac^- (**2**), Pro^- (**3**), Sal^- (**4** and **5**), Bez^- (**6**) and $HMal^-$ (**7**)) cation and one PF_6^- (or Sal^- and Mal^{2-}) anion. The perspective views of the [$Hg(Tab)_2L$]$^+$ cations of **2**−**7** are depicted in Figure 2, and their important bond lengths and angles are compared in Table 2. In each cation of **2**−**7**, the mercury(II) center adopts a distorted seesaw-shaped coordination, coordinated by two sulfur atoms from two Tab moieties and two oxygen atoms from one carboxylate anion (Ac^- for **2**, Pro^- for **3**, Sal^- for **4** and **5**, Bez^- for **6** and $HMal^-$ for **7**).

In the crystals of **2**·0.5H_2O, **3**, **4**·MeOH, **5**·MeOH, and **6**·H_2O, abundant intramolecular and intermolecular hydrogen bonding interactions are observed. For **2**·0.5H_2O, the PF_6^- anions are positioned in-between the [$Hg(Tab)_2(Ac)$]$^+$ cations, which leads to interactions of fluorine atoms with hydrogen atoms of the methyl groups from the Tab ligands and the hydrogen atoms of the acetate anions. For instance, O2 atom of the Ac^- anion has an intramolecular hydrogen-bonding interaction with the hydrogen atom of the phenyl groups [C2···O2] and an intermolecular hydrogen-bonding interaction with the hydrogen atom of methyl groups [C18···O2]. In addition, the F4 atom interacts with the hydrogen atoms from the methyl group of Tab ligand [C9···F4] and the methyl group of acetic anion [C19···F(4)]. All the hydrogen-bonding interactions result in forming a two-dimensional (2D) hydrogen-bonded network extended in the *ab* plane (Figure 3a). Furthermore, these layers are further connected via the hydrogen-bonding interactions between O1 atom of one acetate anion and hydrogen atom of the phenyl groups from one Tab ligand [O1···C5] and hydrogen atom of the methyl groups [O1···C8; O1···C9], between S2 and hydrogen atom from the methyl group [S2···C17], and between F5 and hydrogen atom from the methyl group [F5···C16], generating a three-dimensional (3D) hydrogen-bonded net (Supporting Information, Figure S1).

In the case of **3**, the oxygen atom of the Pro^- anion interacts with the hydrogen atoms of the phenyl or methyl groups of Tab to afford one intramolecular hydrogen-bond [C6···O2] and intermolecular hydrogen-bonds [C12···O2; C16···O2], forming a one-dimensional (1D) chain extending along the *b* axis. Such a chain is further linked by the hydrogen-bonds formed by the fluorine atoms of PF_6^- interactions with the hydrogen atoms of the methyl groups of Tab [C9···F5; C17···F2; C18···F2], thereby giving a 2D network extended along the *ab* plane (Figure 3b).

For **4**·MeOH, there are two intermolecular hydrogen-bonds between O3 and O2 atoms [O3···O2] and between the hydrogen atom from the methyl group and O4 atom from the MeOH molecule [C9···O4], and a set of intermolecular hydrogen-bonds between the hydrogen atom of the hydroxyl group from the MeOH molecule or the hydrogen atom from the methyl group of one Tab ligand and the O1 atom from the Sal^- anion [O4···O1; C16···O1], and between the S1 atom from one Tab ligand and the hydrogen atom from the phenyl group [C3···S1], and between the fluorine atom from one PF_6^- anion and the hydrogen atom from the methyl group of one Tab ligand [C8···F5], giving a 2D layer network

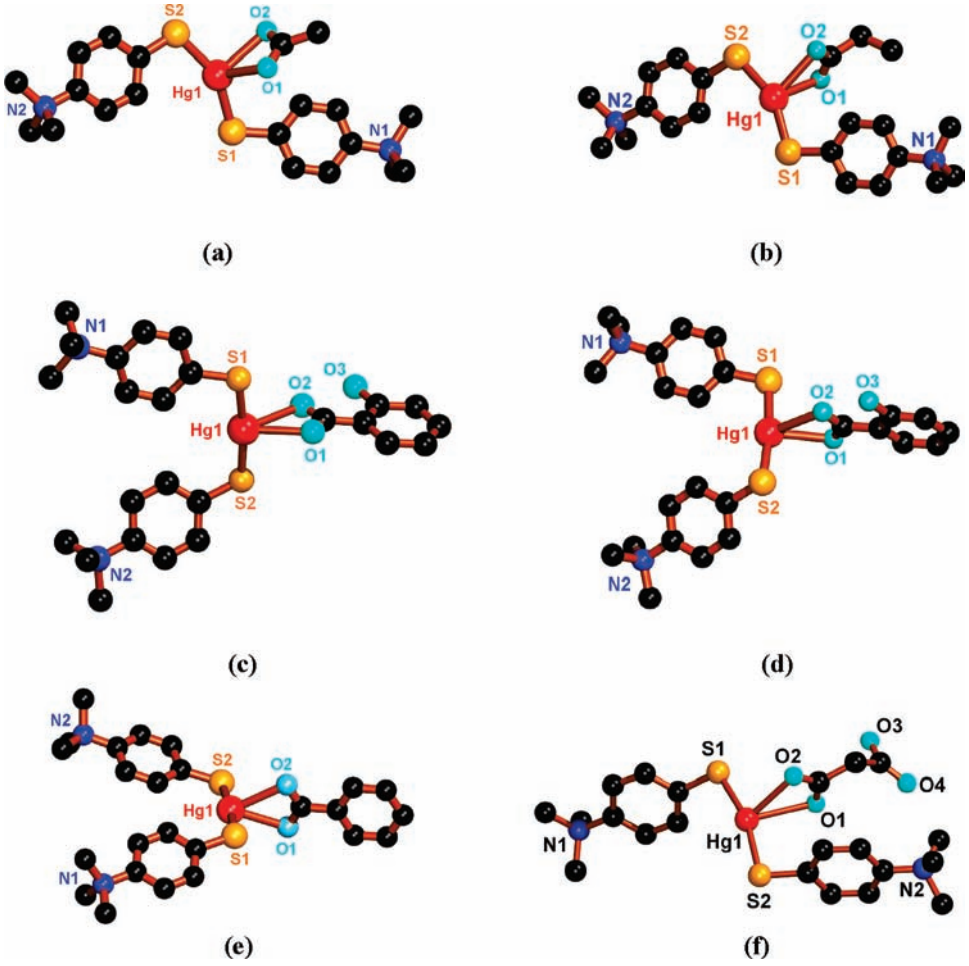

Figure 2. (a) View of the $[Hg(Tab)_2(Ac)]^+$ cation in **2**. (b) View of the $[Hg(Tab)_2(Pro)]^+$ cation in **3**. (c) View of the $[Hg(Tab)_2(Sal)]^+$ cation in **4**. (d) View of the $[Hg(Tab)_2(Sal)]^+$ cation in **5**. (e) View of the $[Hg(Tab)_2(Bez)]^+$ cation in **6**. (f) View of one of the two discrete $[Hg(Tab)_2(HMal)]^+$ cations in **7**. All hydrogen atoms are omitted for clarity.

extending along the *bc* plane (Figure 4a). Furthermore, this layer is connected to its neighboring ones via the intermolecular hydrogen-bonding interactions between the hydrogen atom of the methyl group of one Tab ligand and the fluorine atom from one PF_6^- anion to form a 3D hydrogen-bonded structure (Supporting Information, Figure S2).

In the crystal of **5**·MeOH, one discrete salicylate anion and one MeOH molecule are positioned between the $[Hg(Tab)_2(sal)]^+$ cations. The hydrogen-bonding interactions among the cation, the salicylate anion, and the MeOH solvent molecule afforded eight intramolecular hydrogen-bonds [O3···O2; O6···O5; O7···O4; C7···O4; C7···O5; C12···O7; C16···O7; C18···O7] and three intermolecular hydrogen-bonds [C17···O2; C17···O6; C18···O6], forming a 1D chain running along the *a* axis. Two chains are connected via another three hydrogen-bonding interactions between the O4 atom of the discrete salicylate anion and the hydrogen atom of the methyl group [C7···O4; C8···O4; C9···O4], giving a 1D ribbon extending the *a*-axis (Figure 4b). Each ribbon is further linked by a series of hydrogen-bonds between the oxygen atom of the coordinated salicylate anion and the hydrogen atom of the methyl group [C7···O1; C17···O3; C9···O3], generating a 3D hydrogen-bonded structure (Supporting Information, Figure S3).

In the crystal of **6**·H_2O, the water solvent molecules and the PF_6^- anions are located in-between the $[Hg(Tab)_2(Bez)]^+$ cations. These water molecules are involved in hydrogen bonding interactions [O3···O1; O3···F4]. Furthermore, the fluorine atoms interact with the hydrogen atoms of methyl groups of Tab to afford one intramolecular hydrogen-bond [C9···F2] and two intermolecular hydrogen-bonds [C16···F6; C17···F6], forming a 2D wave-like network extending along the *bc* plane (Figure 4c).

Crystal Structures of 8·2H_2O and 9. X-ray analysis revealed that **8** and **9** hold a similar structure that consists of one $\{[Hg(Tab)_2]_2(\mu\text{-L})\}^{2+}$ (L = Oxa^{2-} for **8**; L = Adi^{2-} for **9**) and two PF_6^- anions. The perspective views of the $\{[Hg(Tab)_2]_2(\mu\text{-Oxa})\}^{2+}$ and the $[Hg(Tab)_2(\mu\text{-Adi})]_2^{2+}$ dications are showed in Figures 5a and 5b. Their pertinent bond lengths and angles are given in Table 2. In the dication of **8** or **9**, two $[Hg(Tab)_2]^{2+}$ fragments are linked by one oxalate or adipate double bridge via four Hg−O bonds to form a dimeric structure with a 2-fold axis going through the Hg1···Hg1A contact (**8**) or a 2-fold axis located at the center of the C21−C21A bond (**9**). Each mercury atom in such a dimer takes a seesaw-shaped coordination, coordinated by two sulfur atoms from Tab ligands and two oxygen atoms from one oxalate or adipate dianion.

Table 2. Selected Bond Lengths (Å) and Angles (deg) in **2**–**11**

Compound **2**			
Hg(1)−S(1)	2.3752(19)	Hg(1)−S(2)	2.3752(19)
Hg(1)−O(1)	2.641(6)	Hg(1)−O(2)	2.506(5)
S(1)−Hg(1)−S(2)	151.22(7)	O(1)−Hg(1)−O(2)	50.31(17)
S(2)−Hg(1)−O(1)	100.37(15)	S(1)−Hg(1)−O(1)	100.09(15)
S(2)−Hg(1)−O(2)	92.57(13)	S(1)−Hg(1)−O(2)	116.10(13)
Compound **3**			
Hg(1)−S(1)	2.360(2)	Hg(1)−S(2)	2.370(2)
Hg(1)−O(1)	2.540(6)	Hg(1)−O(2)	2.582(6)
S(1)−Hg(1)−S(2)	154.54(7)	O(1)−Hg(1)−O(2)	50.41(18)
S(2)−Hg(1)−O(1)	92.47(17)	S(1)−Hg(1)−O(1)	105.94(17)
S(2)−Hg(1)−O(2)	87.06(14)	S(1)−Hg(1)−O(2)	118.18(14)
Compound **4**			
Hg(1)−S(1)	2.335(3)	Hg(1)−S(2)	2.348(3)
Hg(1)−O(1)	2.551(7)	Hg(1)−O(2)	2.857(7)
S(1)−Hg(1)−S(2)	173.36(11)	O(1)−Hg(1)−O(2)	48.59(2)
S(2)−Hg(1)−O(1)	92.4(2)	S(1)−Hg(1)−O(1)	94.0(2)
S(2)−Hg(1)−O(2)	101.53(2)	S(1)−Hg(1)−O(2)	83.91 (2)
Compound **5**			
Hg(1)−S(1)	2.338(2)	Hg(1)−S(2)	2.347(2)
Hg(1)−O(1)	2.553(7)	Hg(1)−O(2)	2.638(6)
S(1)−Hg(1)−S(2)	174.04(8)	O(1)−Hg(1)−O(2)	50.4(2)
S(2)−Hg(1)−O(1)	93.76(17)	S(1)−Hg(1)−O(1)	92.19(18)
S(2)−Hg(1)−O(2)	100.44(17)	S(1)−Hg(1)−O(2)	83.70(17)
Compound **6**			
Hg(1)−S(1)	2.3391(16)	Hg(1)−S(2)	2.3469(16)
Hg(1)−O(1)	2.517(4)	Hg(1)−O(2)	2.842(4)
S(1)−Hg(1)−S(2)	171.91(5)	O(1)−Hg(1)−O(2)	48.39(12)
S(2)−Hg(1)−O(1)	93.94(11)	S(1)−Hg(1)−O(1)	93.89(11)
S(2)−Hg(1)−O(2)	89.13(9)	S(1)−Hg(1)−O(2)	94.57(9)
Compound **7**			
Hg(1)−S(1)	2.354(2)	Hg(1)−S(2)	2.359(2)
Hg(2)−S(3)	2.3550(19)	Hg(2)−S(4)	2.3557(19)
Hg(1)−O(1)	2.745(5)	Hg(1)−O(2)	2.503(5)
Hg(2)−O(3)	2.607(5)	Hg(2)−O(4)	2.780(5)
S(1)−Hg(1)−S(2)	163.65(7)	O(1)−Hg(1)−O(2)	49.43(7)
S(2)−Hg(1)−O(1)	98.93(7)	S(1)−Hg(1)−O(1)	94.64(7)
S(2)−Hg(1)−O(2)	104.52(13)	S(1)−Hg(1)−O(2)	91.23(13)
S(3)−Hg(2)−S(4)	163.26(7)	O(5)−Hg(2)−O(6)	48.54 (7)
S(4)−Hg(2)−O(5)	95.36(12)	S(3)−Hg(2)−O(5)	100.51(12)
S(4)−Hg(2)−O(6)	77.35(12)	S(3)−Hg(2)−O(6)	109.47(12)
Compound **8**			
Hg(1)−S(1)	2.3411(17)	Hg(1)−S(2)	2.3341(17)
Hg(1)−O(1)	2.593(4)	Hg(1)−O(2)	2.770(4)
S(1)−Hg(1)−S(2)	174.37(6)	O(1)−Hg(1)−O(2)	62.46(6)
S(2)−Hg(1)−O(1)	105.98(11)	S(1)−Hg(1)−O(1)	78.44(11)
S(2)−Hg(1)−O(2)	78.89(11)	S(1)−Hg(1)−O(2)	106.46(11)
Compound **9**			
Hg(1)−S(1)	2.364(2)	Hg(1)−S(2)	2.376(2)
Hg(1)−O(1)	2.459(6)	Hg(1)−O(2)	2.653(6)
S(1)−Hg(1)−S(2)	147.68(7)	O(1)−Hg(1)−O(2)	51.23(17)
S(2)−Hg(1)−O(1)	93.22(14)	S(1)−Hg(1)−O(1)	118.85(14)
S(2)−Hg(1)−O(2)	94.47(14)	S(1)−Hg(1)−O(2)	108.36(14)
Compound **10**			
Hg(1)−S(1)	2.4147(15)	Hg(1)−O(1)	2.377(4)
Hg(1)−O(2)	2.644(4)	Hg(1)−O(3)	2.184(4)
S(1)−Hg(1)−S(1A)	93.52(4)	O(1)−Hg(1)−O(2)	48.39(12)
S(2)−Hg(1)−O(1)	93.94(11)	S(1)−Hg(1)−O(1)	93.89(11)
S(2)−Hg(1)−O(2)	89.13(9)	S(1)−Hg(1)−O(2)	94.57(9)
Compound **11**			
Hg(1)−S(1)	2.389(3)	Hg(1)−S(2)	2.401(4)
Hg(1)−O(1)	2.571(9)	Hg(1)−O(3)	2.706(9)
Hg(2)−S(3)	2.393(3)	Hg(2)−S(4)	2.383(4)
Hg(2)−O(5)	2.669(9)	Hg(2)−O(7)	2.572(9)
Hg(1)−N(5)	2.471(10)	Hg(2)−N(6)	2.481(10)
S(1)−Hg(1)−S(2)	155.23(12)	O(1)−Hg(1)−O(3)	130.98(12)
S(2)−Hg(1)−O(1)	102.4(2)	S(1)−Hg(1)−O(1)	92.6(2)
S(2)−Hg(1)−O(3)	92.37(2)	S(1)−Hg(1)−O(3)	92.48(2)
S(3)−Hg(2)−S(4)	158.28(12)	O(5)−Hg(1)−O(7)	133.10(12)
N(5)−Hg(1)−S(1)	110.68(3)	N(5)−Hg(1)−S(2)	93.33(3)
N(5)−Hg(1)−O(1)	67.9(3)	N(5)−Hg(1)−O(3)	64.79(3)
S(4)−Hg(2)−O(5)	88.41(3)	S(3)−Hg(2)−O(5)	96.33(3)
S(4)−Hg(2)−O(7)	100.8(3)	S(3)−Hg(2)−O(7)	91.4(3)
N(6)−Hg(2)−S(3)	104.67(3)	N(6)−Hg(2)−S(4)	96.62(3)
N(6)−Hg(2)−O(5)	65.78(3)	N(6)−Hg(2)−O(7)	67.9(3)

In the crystal of $\mathbf{8}\cdot 2H_2O$, the dications are further connected by the hydrogen-bonding interaction between the F6 atom of one PF_6^- anion and the hydrogen atom from the methyl group [C7···F6; C8···F6], forming a 1D ladder-like chain. This chain is further linked by the hydrogen-bonding interaction between one fluorine atom and the hydrogen atoms from the methyl group [C9···F5; C7···F2], affording a 2D layer structure (Figure 5c).

For **9**, there is one intramolecular hydrogen-bonding interaction between the O atom of the Adi^{2-} anion and the hydrogen atom of the phenyl group with C6 [C6···O1], and eight intermolecular hydrogen -bonding interactions between the oxygen atom of the Adi^{2-} anion and the hydrogen atom of methyl groups with C8 or C16 [C8···O1; C16···O1], or between the fluorine atom of one PF_6^- anion and the H atom of the methyl group with C7, C9, C16 or C18 atom [C7···F1; C9···F1; C9···F4; C9···F5; C16···F5; C18···F2], forming a 3D hydrogen-bonded structure (Figure 5d).

Crystal Structure of 10. An X-ray analysis revealed that **10** has a $[Hg_2(\mu\text{-Tab})_2(\mu\text{-Adi})_2]$ molecule, in which two mercury(II) centers are bridged by two Tab ligands forming a $[Hg(\mu\text{-Tab})_2Hg]^{4+}$ fragment (Figure 6a). Each mercury(II) center in this fragment is further chelated by two adipate anions to form a strongly distorted octahedral coordination geometry. The Hg···Hg separation (3.6210(4) Å) is in good agreement with those in these similar Hg(II)/thiolate dimeric compounds such as $[Hg_2(Tab)_6]Y$ (3.637(2) Å, Y = $(PF_6)_4$; 3.592(2) Å, Y = $(PF_6)Cl_{11}$)[1] and $[Et_4N][Hg_2(SMe)_6]$ (3.631(6) Å),[28] but shorter than those in $[Hg(\mu\text{-Tab})(Tab)Cl]_2Cl_2\cdot H_2O$ (3.996(3) Å), $[Hg(\mu\text{-Tab})(Tab)Cl]_2X_2$ (4.094(5) Å, X = NO_2; 4.020(2) Å, X = NO_3).[1] As shown in Table 2, the mean bridging Hg−S bond length (2.6328(16) Å) is comparable to those in $[Hg(\mu\text{-Tab})(Tab)Cl]_2(NO_2)_2$ (2.693(16) Å), $[Hg_2(Tab)_6]Y$ (2.6895(13) Å, Y = $(PF_6)_4$; 2.6945(12) Å, Y = $(PF_6)Cl_{11}$) and $[Et_4N]_2[Hg_2(SMe)_6]$ (2.668(2) Å), but shorter than those in $[Hg(\mu\text{-Tab})(Tab)Cl]_2Cl_2\cdot H_2O$ (2.7496(16) Å) and $[Hg(\mu\text{-Tab})(Tab)Cl]_2(NO_2)_2$ (2.755(2) Å). Topologically, each resulting $[Hg_2(\mu\text{-Tab})_2(\mu\text{-Adi})_2]$ molecule works as a planar four-connecting node, which is interconnected to its four equivalent ones via four adipate dianions, thereby forming a unique 2D network extending along the bc plane (Figure 6b).

(28) Bowmaker, G. A.; Dance, I. G.; Dobson, B. C.; Rogers, D. A. *Aust. J. Chem.* **1984**, *37*, 1607.

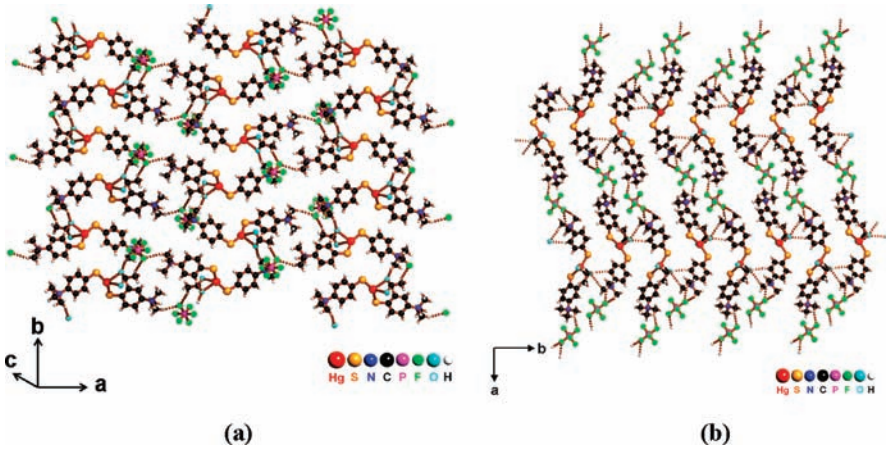

Figure 3. (a) 2D network extended along the *ab* plane formed via hydrogen-bonding interactions in **2**·0.5H_2O (looking down the *c* axis). (b) 2D network extended along the *ab* plane formed via hydrogen bonding interactions in **3** (looking down the *c* axis).

Crystal Structure of 11·2.5H_2O. Compound **11**·2.5H_2O crystallizes in the orthorhombic space group *Pbca* and its asymmetric unit consists of two crystallographically independent [Hg(Tab)$_2$(Meida)] molecules and five H_2O solvent molecules. Because the two [Hg(Tab)$_2$(Meida)] molecules are structurally similar, only one of them is presented in Figure 7a. The pertinent bond lengths and angles of the two molecules are compared in Table 2. Each [Hg(Tab)$_2$] fragment in two molecules is further chelated with one nitrogen and two oxygen atoms from one Meida ligand to form a rare distorted square pyramidal coordination geometry. The average Hg−S bond distance of 2.395(2) Å is comparable to these of the aforementioned Hg/Tab compounds. The mean Hg−N bond length (2.476(10) Å) is comparable to that of the complex containing similar HgS_2O_2N coordination environment such as [Hg(SMe)(CH_3COO)(MePy)]$_n$ (2.418(4) Å), but shorter than that in [Hg(SEt)(CH_3COO)(Py)]$_n$ (2.656(2) Å),[29a] and longer than those of the corresponding ones of some five-coordinated Hg(II) compounds such as [HgI(Pic)(Hpic)] (2.298(3) Å; Hpic = picolinic acid)[8a] and [HgL(ClO_4)$_2$] (2.365(2) Å; L = 3,11,19-trithia[3.3.3]pyridinophane).[29b] The mean Hg−O bond length of 2.637(9) Å is slightly somewhat longer than those in [Hg(SMe)(CH_3-COO)(MePy)]$_n$ (2.545(3) Å) and [Hg(SEt)(CH_3COO)(Py)]$_n$ (2.510(2) Å).[29a] In the crystal of **11**·2.5H_2O, two [Hg(Tab)$_2$-(Meida)] molecules are arranged around 2-fold screw axes to a pseudochiral dimeric species [Hg(Tab)$_2$(Meida)]$_2$.

In **11**·2.5H_2O, there exist abundant intra- and intermolecular hydrogen-bonding interactions among the [Hg(Tab)$_2$(Meida)] molecule and water solvent molecules. There are five intramolecular hydrogen-bonding interactions between sulfur atom of the Tab ligand and the hydrogen atom of the methyl group with C17 [C17···S1] and C27 [C27···S3], between oxygen atoms of the Meida ligand and hydrogen atoms from solvated water molecules O8 [O11···O8] or from methyl groups of Tab ligand O7 [C17···O7], and between the oxygen atoms and the hydrogen atoms from water molecules O13 [O13···O12]. The intermolecular interactions [C17···O6; C26···O5; C25···O5; C26···S3; O44···O13; C34···O2; C36···O1] led to the formation of chain structure extended along the *b* axis (Figure 7b). Because of the existence of solvated water molecules in the lattice, these chains are further linked via the hydrogen bonding interactions occurred between hydrogen atoms from water molecules and oxygen atoms from Meida ligands [O9···O2; O9···O4; O10···O6; O10···O8; O11···O8] or oxygen atoms from water molecules [O12···O11; O12···O10; O13···O4] or between hydrogen atoms from methyl groups of the Tab ligands and oxygen atoms from the Meida ligands [C7···O4; C16···O8] into a 3D hydrogen-bonded structure (Supporting Information, Figure S4).

Variations in the Configurations of [Hg(Tab)$_2$] Units of 2−11. Because of the coordination of carboxylate ligands at the Hg center, the original *trans*-configuration of the [Hg(Tab)$_2$] unit of **1** is changed in **2**−**11**. First, two Tab ligands rotate around the S−Hg−S line by some degrees. For instance, in **4**−**6** and **8**, two Tab ligands turn around the S−Hg−S string by about 150° with the dihedral angles between N1S1Hg1 and N2S2Hg1 planes of 23.8° (**4**), 38.5° (**5**), 26.6° (**6**) and 35.6° (**8**). However, the two Tab groups in **11** turn by about 90° around the S1−Hg1−S2 line or S3−Hg2−S4 line, which makes the two Tab groups be oriented almost in the vertical direction with a dihedral angle between the similar planes being 76.75(2)° or 78.59(2)°. In the case of **2**, **3**, **7**, and **9**, the two Tab units almost retain the original *trans*-configuration, with some slight rotation of both groups around the S−Hg−S line because their dihedral angles are 145.5° (**2**), 160.4° (**3**), 156.8°, and 157.6° (**7**), and 164.2° (**9**). Second, the two Tab groups swing from left to right along the S−Hg−S line. Such a swing causes the deviation of the two N(Tab)−S−Hg angles in **2**−**11** from those of the corresponding ones in **1** (104.16°). The steric hindrance among the carboxylate anions and two Tab groups enlarges the N(Tab)−S−Hg angle and both Tab groups thus understandably swing outward. The N(Tab)−S−Hg angles are 110.924°/112.584° (**2**), 110.425°/111.745° (**3**), 109.324°/109.401° (**4**), 107.961°/107.369° (**5**), 110.039°/109.465° (**6**), 103.38°/109.25°/111.43°/108.06° (**7**), 111.501°/109.553° (**8**), 112.52°/110.63° (**9**), and 111.825°/104.043°/109.084°/106.689° (**11**). In the cases of **7** or **11**, one N(Tab)−S−Hg angle is smaller than that in **1**, suggesting that the two Tab groups slightly swing inward. Third, the rotation of the two phenyl groups of the Tab ligands in **2**−**9** and **11** is observed. As described previously, the two phenyl groups of **1** are in a parallel position. Both groups in **2**−**9** and **11** are

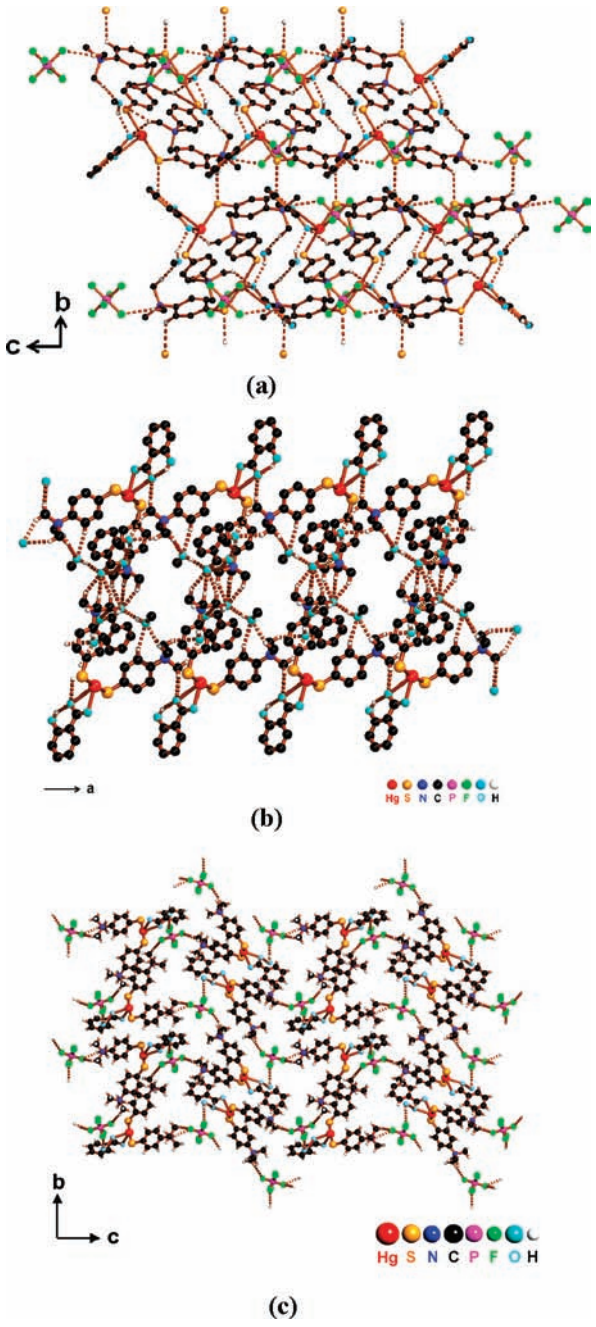

Figure 4. (a) 2D network of **4**·MeOH (looking long the *a* axis) extending along the *bc* plane. (b) View of a section of the 1D ribbon formed via hydrogen-bonding interactions in **5**·MeOH (extending along the *a* axis). (c) 2D network of **6**·H_2O extending along the *bc* plane. All hydrogen atoms except those related to hydrogen bonding interactions are omitted for clarity.

found to rotate by some degrees along the S−N(Tab) line to deviate from the original parallel position. The dihedral angle between the phenyl groups of the Tab ligands in **2**−**9** and **11** are 13.4° (**2**), 11.8° (**3**), 16.3° (**4**), 18.3° (**5**), 16.4° (**6**), 12.5°/75.6° (**7**), 11.6° (**8**), and 6.7° (**9**), respectively. In the case of **11**, two Tab ligands are almost in vertical positions with the dihedral angle of 87.4° and 80.4°. Fourthly, for **4**−**6** and **8**, their S−Hg−S angles, 173.36(11)° for **4**, 174.04(8)° for **5**, 171.91(5)° for **6**, and 174.37(6)° for **8**, are found to deviate slightly from 180.00° in **1**. However, the S−Hg−S angles, 151.22(7)° for **2**, 154.54(7)° for **3**, 163.65(5)°/163.67(5)° for **7**, and 147.68(**7**)° for **9**, and 155.23(12)°/158.28(12)° for **11**, remarkably deviate from 180.00° in **1**. Finally, although the anion basicity seems of no effect on the types of structures, there is a correlation between the anion structure and the types of structures observed. For example, the two Tab units in **2**, **3**, and **7** almost retained their original *trans* configuration in **1** when its mercury center is bound by alkyl carboxylate anions such as Ac^-, Pro^-, Mal^{2-} anions while those in **4**, **5**, and **6** adopted the *cis* configuration when the mercury center in **1** is bound by aryl carboxylate anions like Sal^- and Bez^- anions.

The Hg−S bond lengths and S−Hg−S angles of **2**−**11** are also changed because of the coordination of carboxylate ligands at the Hg center (Table 2). The average Hg−S bond distances of 2.3752(19) Å for **2**, 2.365(2) Å for **3**, 2.342(3) Å for **4**, 2.343 (2) Å for **5**, 2.343 (16) Å for **6**, 2.356 (2) Å for **7**, 2.3376(17) Å for **8**, and 2.370 (2) Å for **9** are longer than that of **1** (2.331(3) Å). The longest Hg−S bond length is observed in **6**. As shown in Table 3, these mean Hg−S bond lengths are shorter that those of the four-coordinated mercury(II)/thiolate compounds such as $[Hg(4\text{-}SpyH)_2(4\text{-}Spy)_2]$ (2.520(2)−2.577(3) Å, 4-Spy = pyridine-4-thiolate) and $[HgL_4]^-$ (2.527(2)−2.552(2) Å for L = 4-chlorobenzenethiolate; 2.520(3) Å for L = 2-phenylbenzenethiolate; 2.551(3) Å for L = 2-(*N*-methylcarbamoyl)phenylthiolate),[30] but are close to those in Hg/Tab/N-donor ligand compounds and EXAFS data for the tricoordinated mercury centers in Hg-MerR,[31] Hg_7-MT,[32] and Hg_{18}-MT.[33] We assumed that the Hg−S bond lengths in the range of 2.338(2)−2.415(2) Å are special for the seesaw-shaped $[HgS_2O_2]$ coordination geometry. The Hg−O bond lengths vary in a relatively large range. The shortest and longest Hg−O bond lengths are observed in **10** (2.184(4) Å) and **4** (2.857(7) Å), respectively. The mean Hg−O bond lengths, 2.574(5) Å for **2**, 2.561(6) Å for **3**, 2.704(7) Å for **4**, 2.5955 Å for **5**, 2.6795(4) Å for **6**, 2.659(4) Å for **7**, 2.6815(4) Å for **8**, 2.556(6) Å for **9**, 2.514(4) Å for **10**, and 2.629(9) Å for **11** are comparable to those found in $[Hg(SEt)(Ac)Py]_n$ (2.510(4) Å),[29] $[Hg(SMe)(Ac)(\mu\text{-}MePy)]_n$ (2.591(5) Å),[34] and $[Hg(SMe)(Ac)Py]_n$ (2.555(3) Å),[35a] and longer than that in $[Hg(2\text{-}Spy)(Ac)]_n$ (2.483(4) Å).[35b] Most of these Hg−O bonds may be considered as a coordinative bond. However, the longer Hg−O bonds like those in **4** (2.857(7) Å) are very weak, which implies that the mercury atoms may form ionic bonds with the added carboxylates. Even in such a case, the geometry of the mercury(II) center in **4** still got somewhat changed relative to that of **1**. Therefore this may provide some implication that the geometry of the

(29) (a) Canty, A. J.; Raston, C. L.; White, A. H. *Aust. J. Chem.* **1979**, *32*, 311. (b) Vetrichelvan, M.; Lai, Y. H.; Mok, K. F. *Eur. J. Inorg. Chem.* **2004**, 2086.
(30) (a) Silver, A.; Koch, S. A.; Millar, M. *Inorg. Chim. Acta* **1993**, *9*, 205. (b) Choudhury, S.; Dance, I. G.; Guerney, P.; Rae, A. D. *Inorg. Chim. Acta* **1983**, *70*, 227. (c) Kato, M.; Kojima, K.; Okamura, T.; Yamamoto, H.; Yamamura, T.; Ueyama, N. *Inorg. Chem.* **2005**, *44*, 4037. (d) Anjali, K. S.; Vittal, J. J.; Dean, P. A. W. *Inorg. Chim. Acta* **2003**, *79*, 351. (e) Manceau, A.; Nagy, K. L. *Dalton Trans.* **2008**, 1421.
(31) (a) Penner-Hahn, J. E.; Tsang, H. T.; O'Halloran, T. V.; Wright, J. *Physica B* **1989**, *158*, 117. (b) Jaliehvand, F.; Leung, B. O.; Izadifard, M.; Damian, E. *Inorg. Chem.* **2006**, *45*, 66.
(32) Hasnain, S. S. In *Synchrotron Radiation in Chemistry and Biology II*; Mandelkow, E., Ed.; Springer-Verlag: New York, 1988; p 73.
(33) (a) Jiang, D. T.; Heald, S. M.; Sham, T. K.; Stillman, M. J. *J. Am. Chem. Soc.* **1994**, *116*, 11004. (b) Lu., W. H.; Kasrai, M.; Bancroft, G. M.; Stillman, M. J.; Tan, K. H. *Inorg. Chem.* **1990**, *29*, 2561.
(34) Puff, H.; Sievers, R.; Elsner, G. *Z. Anorg. Allg. Chem.* **1975**, *413*, 37.
(35) (a) Canty, A. J.; Raston, C. L.; White, A. H. *Aust. J. Chem.* **1978**, *31*, 677. (b) Wang, S. N.; Junior, J. P. F. *Inorg. Chem.* **1989**, *28*, 2615.

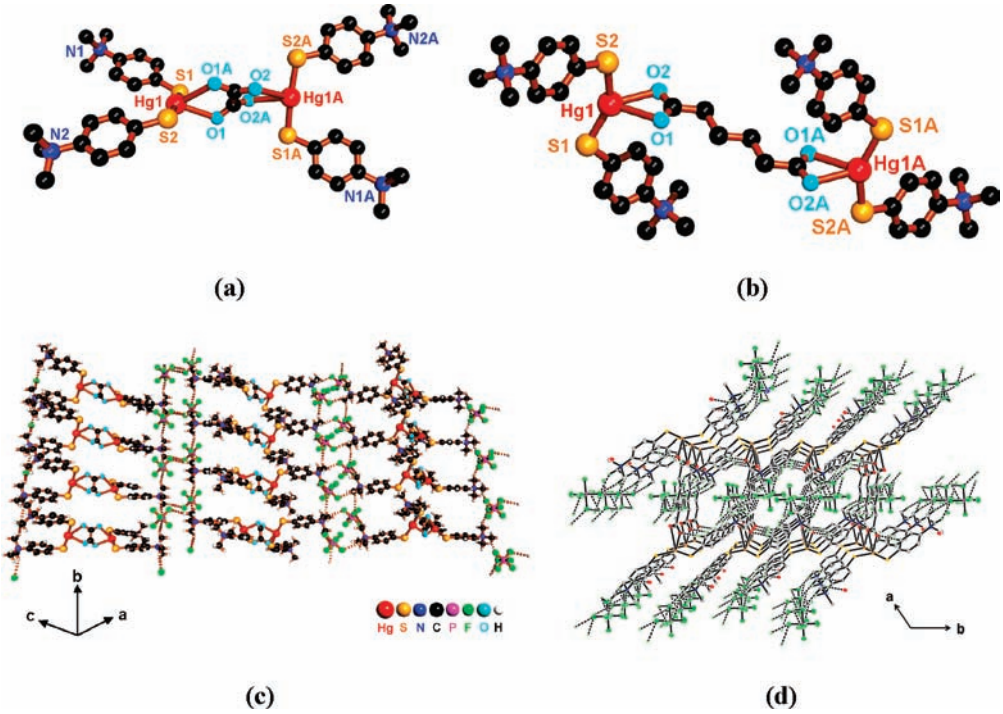

Figure 5. (a) View of the $\{[Hg(Tab)_2]_2(\mu\text{-Oxa})\}^{2+}$ dication of **8**. Symmetry transformations used to generate equivalent atoms, A: $-x, y, -z + 1/2$. (b) View of the $[Hg(Tab)_2(\mu\text{-Adi})]_2^{2+}$ dianion of **9**. Symmetry transformations used to generate equivalent atoms, A: $-x, 1/2 + y, 1/2 - z$. (c) 2D layer structure formed by the hydrogen-bonding interactions in $\mathbf{8}\cdot 2H_2O$. (d) View of a 3D hydrogen-bonded structure of **9** looking along the *c* axis. All hydrogen atoms except those involved in hydrogen bonding interactions are omitted for clarity.

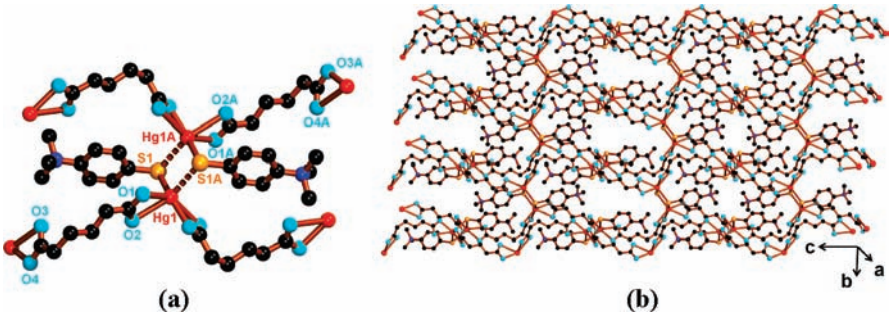

Figure 6. (a) View of the dimeric $[Hg_2(\mu\text{-Tab})_2(\mu\text{-Adi})_2]$ fragment in **10**. (b) View of the 2D network of **10** extending along the *bc* plane. All hydrogen atoms have been omitted for clarity.

mercury(II) atom in the mercury(II)-containing proteins may be affected by the added anions even though the mercury atoms form ionic bonds with them.

Conclusions

In this paper, we have demonstrated the interesting reactivity of the precursor complex **1** toward alkyl carboxylic acids (acetic acid, propionic acid) and aryl acids (benzoic acid, salicylic acid) or dicarboxylic acids (oxalic acid, malonic acid, adipic acids, methylimindiazole acid), and successful isolation of 10 new mercury(II)-Tab-carboxylate compounds (**2**−**11**). According to their X-ray analysis, the linear coordination geometry of mercury(II) center in **1** is converted into a seesaw-shaped coordination (**2**−**9**), a distorted octahedral coordination (**10**), or a distorted square pyramidal five-coordination (**11**) when the Hg center is coordinated by these carboxylate anions. The latter two geometries for the mercury(II) centers in **10** and **11** are uncommon in mercury thiolate chemistry. Similar to the mercury-Tab-amine compounds, the *trans* configuration of the dication of **1** is also found to undergo changes in **2**−**11** in three ways: the rotation of the two Tab groups around the S−Hg−S line, the swing of the two Tab groups along the S−Hg−S line, and the rotation of the two phenyl groups of the Tab ligands along the S−N(Tab) line. These configuration variations result in the changes of the Hg−S bond lengths and the S−Hg−S bond angles in **2**−**11**. Because the Hg−S bond lengths of 2.334−2.401 Å in **2**−**9** do not fall among those of compounds containing the tetrahedrally coordinated mercury(II) atoms, they may be established for the seesaw-shaped four-coordinated $[HgS_2O_2]$. In addition, the UV−vis absorption data of **2**−**11** might correlate with their structural features to some extent when compared with those of the existing mercury(II)-thiolate compounds. According to these results, we could derive two important implications for the related biological systems. One is that the geometry of the mercury(II) sites of mercury(II)-MerR and mercury(II)-MT might be changed when they encounter naturally existing carboxylic acids or amino acids from these proteins, which is of importance in understanding the structural data of mercury(II)-MerR and

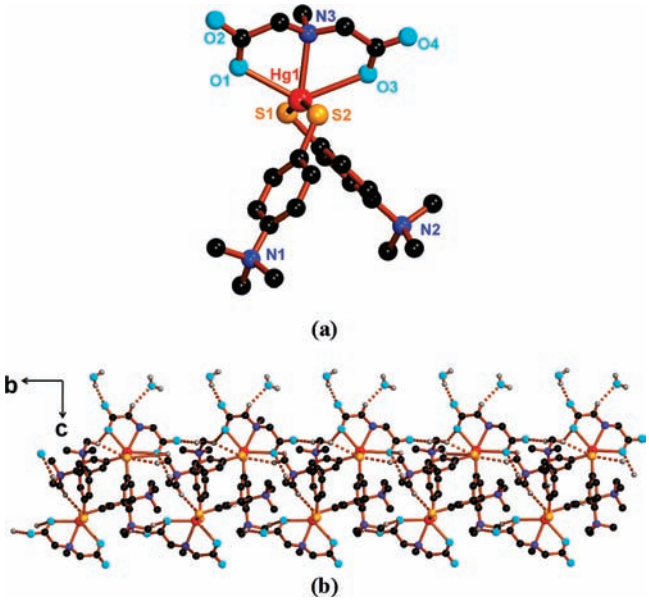

Figure 7. (a) View of the molecular structure of $[Hg(Tab)_2(Meida)]$ in **11**. All hydrogen atoms and H_2O molecules are omitted for clarity. (b) View of the chain structure formed via hydrogen bonding interactions in **11**·2.5H_2O. All hydrogen atoms except those involved in hydrogen interactions or H_2O molecules are omitted for clarity.

Table 3. Hg−S and Hg−O Bond Lengths (Å) in **1**−**11** and Other Mercury(II) Thiolate or Carboxylate Compounds

compound	Hg−S	Hg−O	ref.
$[Hg(Cys)_2]^{2-a}$	2.32−2.36		36a
$[Hg(Cys)_3]^{4-}$	2.43−2.45		36b
$[Hg(HCys)(H_2Cys)]Cl·0.5H_2O$	2.329−2.355		14
Hg-MerR [b]	2.42−2.43		31a, 31b
Hg_7-MT[c]	2.33−2.42		36a
Hg_{18}-MT	2.41−2.42		33
$[Hg_2(Ac)_3(NO_3)]_n$		2.464	6
$[Hg(nico)Br]_n$[d]		2.415	7
Hg(α-picolinate)$_2$		2.481	8a
		2.471	8b
$[Hg(pydc)_2]$(piperazinium)·$6H_2O$ [e]		2.470	9a
$\{(Hpyda)_2[Hg(pydc)Cl)]_2·2H_2O\}_n$[f]		2.638	9b
$[Hg(pydc)I_2]L$[g]		2.586	9c
$[Hg_4(proline)_2Cl_8]$		2.651	19b
MeHg(alanine)		2.726	21a
$[Hg_{12}(alanine)(NO_3)_8]·2H_2O$		2.122−2.225	21c
1	2.331(3)		1a
2	2.3752(19)	2.574(5)	this work
3	2.365(2)	2.561(6)	this work
4	2.342(3)	2.704(7)	this work
5	2.343(2)	2.5955	this work
6	2.343(16)	2.6795(4)	this work
7	2.356(2)	2.659(5)	this work
8	2.3376(17)	2.6815 (4)	this work
9	2.370(2)	2.556(6)	this work
10	2.4147(15)	2.514(4)	this work
11	2.3915	2.629(9)	this work

[a] Cys = cysteine. [b] MerR = metalloregulatory protein. [c] MT = metallothionein. [d] nico = nicotinate. [e] pyda =2,6-pyridinediamine. [f] H_2pydc = 2,6-pyridinedicarboxylic acid. [g] L = 1,1′-(butane-1,4-diyl)bis(1*H*-benzimidazol-3-ium).

mercury(II)-MT derived from EXAFS, NMR, UV−vis, and Raman spectroscopic studies. The other is that during detoxification, the coordination geometry of mercury(II) that is transferred or released might vary from linear to T-shaped to seesaw-shaped to square pyramidal to octahedral coordination geometry. The biological anions might play an important role in these transformations because they work as multitopic ligands to bind the mercury centers and make the coordination surrounding of the mercury(II) center changed. We are currently extending this work by investigating the reactions of **1** with the transition or main group metal ions (Zn(II), Cd(II), Hg(II), Pb(II)).

Experimental Section

General Procedures. Compound **1** was prepared according to the literature method.[1a] Other chemicals and reagents were obtained from commercial sources and used as received. All Solvents were predried over activated molecular sieves and refluxed over appropriate drying agents and freshly distilled prior to use. IR spectra were recorded on a Varian 1000 FT-IR spectrometer as KBr disks (4000−400 cm^{-1}). UV−vis spectra were measured on a Varian 50 UV−visible spectrophotometer. Elemental analyses for C, H, and N were performed on a Carlo-Erba CHNO-S microanalyzer. ^{1}H NMR spectra were recorded at ambient temperature on a Varian UNITYplus-400 spectrometer. ^{1}H NMR chemical shifts were referenced to the DMSO-d_6 signal.

Synthesis. $[Hg(Tab)_2(Ac)](PF_6)·0.5H_2O$ (2·0.5H_2O). To a solution of **1** (0.825 g, 1 mmol) in MeCN (15 mL) was added a solution containing acetic acid (0.124 g, 2 mmol) in H_2O (2 mL). The resulting colorless solution was neutralized by Et_3N to pH = 7 and stirred at ambient temperature for 0.5 h and filtered. Diethyl ether (40 mL) was layered onto the filtrate at ambient temperature for two weeks, forming colorless blocks of **2**·0.5H_2O, which were collected by filtration, washed by Et_2O and dried in vacuo. Yield: 0.67 g (77% based on Hg). Anal. Calcd. for $C_{20}H_{30}F_6HgN_2O_{2.5}PS_2$: C, 32.11; H, 4.04; N, 3.74. Found: C, 32.32; H, 3.83; N, 3.89. IR (KBr disk): 3406 (br), 3041 (w), 2972 (w), 1576 (m), 1552 (s), 1490 (s), 1405 (m), 1128 (m), 1010 (m), 962 (w), 842 (s), 745 (w), 654 (w), 559 (s) cm^{-1}. UV−vis (MeCN, λ_{max}(nm (ε M^{-1} cm^{-1}))): 268 (97000). ^{1}H NMR (400 MHz, $(CD_3)_2SO$): δ 7.51−7.66 (m, 8H, Ph), 3.54 (s, 18H, NMe_3), 1.69 (s, 3H, Me).

$[Hg(Tab)_2(Pro)](PF_6)$ (3). Compound **3** was prepared as colorless plates in a manner similar to that described for the preparation of **2**, using **1** (0.825 g, 1 mmol) in 15 mL of MeCN and propanoic acid (0.150 g, 2 mmol) in H_2O (2 mL). Yield: 0.69 g (92% based on Hg). Anal. Calcd. for $C_{21}H_{31}F_6HgN_2O_2PS_2$: C, 33.49; H, 4.15; N, 3.72. Found: C, 33.52; H, 3.97; N, 3.81. IR (KBr disk): 3028 (w), 2984 (2), 1575 (m), 1547 (s), 1491 (s), 1406 (m), 1363 (w), 1129 (m), 1011 (w), 960 (m), 838 (s), 745 (w), 632 (w), 559 (s) cm^{-1}. UV−vis (MeCN, λ_{max}(nm (ε M^{-1} cm^{-1}))): 267 (84000). ^{1}H NMR (400 MHz, $(CD_3)_2SO$): δ 7.51−7.65 (m, 8H, Ph), 3.52 (s, 18H, NMe_3), 1.88−1.93 (m, 2H, CH_2), 0.89−0.93 (m, 3H, Me).

$[Hg(Tab)_2(Sal)](PF_6)·MeOH$ (4·MeOH). Compound **4**·MeOH was prepared as colorless needles in a manner similar to that described for the preparation of **2**, using **1** (0.825 g, 1 mmol) in 15 mL of MeCN and salicylic acid (0.190 g, 1 mmol) in MeOH (3 mL) and H_2O (1 mL). Yield: 0.73 g (87% based on Hg). Anal. Calcd. for $C_{26}H_{35}F_6N_2HgO_4PS_2$: C, 36.77; H, 4.15; N, 3.30. Found: C, 36.54; H, 4.36; N, 3.47. IR (KBr disk): 3429 (m), 3043(w), 1624 (w), 1585 (w), 1557 (w), 1488 (m), 1457 (w), 1380 (w), 1355 (w), 1258 (w), 1126 (w), 1010 (w), 959 (w), 840 (s), 707 (w), 667 (w), 559 (m) cm^{-1}. UV−vis (MeCN, λ_{max}(nm (ε M^{-1} cm^{-1}))): 261 (86000). ^{1}H NMR (400 MHz, $(CD_3)_2SO$): δ 7.70−7.72 and 7.58−7.60 (m, 8H, Ph in Tab), 7.62−7.64 (m, 1H, Ph in Sal), 7.10−7.15 (m, 1H, Ph in Sal), 6.57−6.62 (m, 2H, Ph in Sal), 4.08 (br, 1H, OH), 3.53 (s, 18H, NMe_3).

$[Hg(Tab)_2(Sal)](Sal)·MeOH$ (5·MeOH). Compound **5**·MeOH was prepared as long colorless needles in a manner similar to that described for the preparation of **4**, using **1** (0.825 g, 1 mmol) in 15 mL of MeCN and salicylic acid (0.379 g, 2 mmol) in MeOH

Table 4. Crystallographic Data for **2**·0.5H_2O, **3**, **4**·MeOH, **5**·MeOH, **6**·H_2O, **7**·H_2O, **8**·2H_2O, **9**, **10**, and **11**·2.5H_2O

	2·0.5H_2O	**3**	**4**·MeOH	**5**·MeOH	**6**·H_2O	**7**·H_2O	**8**·2H_2O	**9**	**10**	**11**·2.5H_2O
chemical formula	$C_{40}H_{60}F_{12}Hg_2N_4O_5P_2S_4$	$C_{21}H_{31}F_6HgN_2O_2PS_2$	$C_{36}H_{34}F_6HgN_2O_4PS_2$	$C_{33}H_{40}HgN_2O_7S_2$	$C_{50}H_{64}F_{12}Hg_2N_4O_5P_2S_4$	$C_{22.5}H_{32}HgN_2O_7S_2$	$C_{38}H_{56}F_{12}Hg_2N_4O_6P_2S_4$	$C_{42}H_{60}F_{12}Hg_2N_4O_4P_2S_4$	$C_{15}H_{21}HgNO_4S$	$C_{23}H_{38}HgN_3O_{6.5}S_2$
fw	1496.32	753.18	848.25	841.40	1620.45	1414.46	1484.27	1504.34	511.99	1450.59
cryst. syst.	monoclinic	monoclinic	monoclinic	triclinic	orthorhombic	triclinic	monoclinic	monoclinic[d]	orthorhombic[e]	orthorhombic[f]
space group	$P2_1/c$	$P2_1/a$	$P2_1/c$	$P\bar{1}$	$Pbcn$	$P\bar{1}$	$C2/c$	$P2_1/c$	$Pbca$	$Pbca$
a (Å)	15.826(3)	14.426(3)	14.800(3)	9.6245(19)	23.676(5)	9.6776(19)	33.884(7)	14.530(3)	17.336(2)	14.639(3)
b (Å)	13.326(3)	12.697(2)	22.947(5)	12.634(3)	9.0739(18)	15.754(3)	7.6754(15)	13.088(3)	10.1793(12)	20.439(4)
c (Å)	13.278(3)	15.187(3)	9.0456(18)	14.069(3)	28.876(6)	18.912(4)	22.789(5)	14.478(3)	18.672(2)	37.011(7)
α (deg)				80.34(3)	108.51(3)					
β (deg)	102.42(3)	104.718(4)	93.12(3)	88.57(3)		98.36(3)	119.33(3)	106.12(3)		
γ (deg)				89.27(3)		105.00(3)				
V (Å^3)	2734.8(11)	2690.5(9)	3067.4(11)	1685.9(7)	6204(2)	2558.2(12)	5167(2)	2645.0(11)	3295.0(6)	11074(4)
Z	2	4	4	2	4	2	4	2	8	8
T/K	193(2)	193(2)	173(2)	193(2)	213(2)	193(2)	193(2)	193(2)	193(2)	223(2)
D_{calcd} (g cm^{-3})	1.817	1.859	1.839	1.658	1.735	1.836	1.908	1.889	2.064	1.908
λ (Mo Kα) (Å)	0.71073	0.71070	0.71073	0.71073	0.71073	0.71073	0.71073	0.71073	0.71070	0.71073
μ (cm^{-1})	59.02	59.99	52.11	47.38	52.11	62.25	62.48	61.02	94.85	62.48
$2\theta_{max}$ (deg)	50.7	50.7	50.7	50.7	50.7	50.7	50.7	50.7	50.7	55.0
no. of reflns collected	26202	25925	28905	16711	56687	25206	24324	25091	30054	34031
no. of unique reflns	4986	4923	5382	6148	5667	9316	4723	4827	3016	9559
R_{int}	0.0660	0.0691	0.1221	0.0466	0.0552	0.0459	0.0551	0.0998	0.0483	0.0669
no. of obsd. reflns ($I > 2.00\sigma(I)$)	4454	4223	4526	5482	5113	7843	3880	4122	2862	8005
no. of variables	333	312	387	416	367	618	322	322	203	652
R^a	0.0493	0.0570	0.1121	0.0411	0.0575	0.0467	0.0429	0.0565	0.0388	0.0742
wR^b	0.1145	0.0957	0.2648	0.0773	0.1296	0.0895	0.0635	0.1335	0.0608	0.1649
GOF[c]	1.164	1.273	1.063	1.040	1.226	1.184	1.163	1.083	1.120	1.090

[a] $R = \sum||F_o| - |F_c||/\sum|F_o|$. [b] $wR = \{\sum w(F_o^2 - F_c^2)^2/\sum w(F_o^2)^2\}^{1/2}$. [c] GOF = $\{\sum[w(F_o^2 - F_c^2)^2]/(n-p)\}^{1/2}$, where n = number of reflections and p = total numbers of parameters refined. [d] Crystal size (mm^3): 0.50 × 0.30 × 0.18. [e] Crystal size (mm^3): 0.40 × 0.31 × 0.21. [f] Crystal size (mm^3): 0.35 × 0.24× 0.20.

(5 mL) and H_2O (2 mL). Yield: 0.66 g (78% based on Hg). Anal. Calcd. for $C_{33}H_{40}HgN_2O_7S_2$: C, 47.10; H, 4.79; N, 3.33. Found: C, 47.25; H, 4.41; N, 3.62. IR (KBr disk): 3420 (m), 3041 (w), 1624 (w), 1585 (m), 1488 (s), 1455 (m), 1384 (s), 1301 (w), 1257 (w), 1127 (w), 1085 (w), 1035 (w), 1010 (w), 950 (w), 857 (s), 758 (w), 706 (w), 667 (w), 558 (w) cm^{-1}. UV−vis (MeCN, λ_{max}(nm (ε M^{-1} cm^{-1}))): 264 (104000). ^1H NMR (400 MHz, $(CD_3)_2SO$): δ 7.70−7.72 and 7.59−7.61 (m, 4H, Ph in Tab), 7.62−7.65 (m, 2H, Ph in sal), 7.09−7.13 (m, 2H, Ph in sal), 6.55−6.60 (m, 4H, Ph in sal), 4.05 (br, 1H, OH), 3.54 (s, 9H, NMe_3).

[Hg(Tab)$_2$(Bez)](PF$_6$)·H$_2$O (6·H$_2$O). Compound **6**·H_2O was prepared as colorless prisms in a manner similar to that described for the preparation of **2**, using **1** (0.825 g, 1 mmol) in 15 mL of MeCN and benzoic acid (0.244 g, 2 mmol) in MeOH (4 mL) and H_2O (2 mL) at pH = 8. Yield: 0.70 g (86% based on Hg). Anal. Calcd. for $C_{25}H_{32}F_6HgN_2O_{2.5}PS_2$: C, 37.06; H, 3.98; N, 3.46. Found: C, 37.33; H, 3.71; N, 3.75. IR (KBr disk): 3415 (m), 1594 (w), 1548 (w), 1489 (s), 1375 (m), 1126 (w), 1085 (w), 1010 (w), 958 (w), 838 (s), 723 (w), 676 (w), 559 (m) cm^{-1}. UV−vis (MeCN, λ_{max}(nm (ε M^{-1} cm^{-1}))): 267 (148800). ^1H NMR (400 MHz, $(CD_3)_2SO$): δ 7.55−7.65 (m, 8H, Ph in Tab), 7.80−7.82 (m, 2H, Ph in Bez), 7.29−7.37 (s, 3H, Ph in Bez), 3.49 (s, 18H, NMe_3).

[Hg(Tab)$_2$(HMal)](Mal)$_{0.5}$·H$_2$O (7·H$_2$O). Compound **7**·$2H_2O$ was prepared as colorless blocks in a manner similar to that described for the preparation of **2**, using **1** (0.825 g, 1 mmol) in 15 mL of MeCN and malonic acid (0.208 g, 2 mmol) in H_2O (5 mL). Yield: 0.58 g (82% based on Hg). Anal. Calcd. for $C_{22.5}H_{32}HgN_2O_7S_2$: C, 38.21; H, 4.56; N, 3.96. Found: C, 38.42; H, 3.73; N, 3.83. IR (KBr disk): 3462 (m), 3033 (m), 2974 (m), 1735 (s), 1584(m), 1490 (s), 1420 (w), 1127 (w), 1010 (m), 958 (m), 838 (m), 747 (w), 559 (w) cm^{-1}. UV−vis (MeCN, λ_{max}(nm (ε M^{-1} cm^{-1}))): 264 (73000). ^1H NMR (400 MHz, D_2O): δ 7.53−7.65 (m, 16 H, Ph), 3.51 (s, 18H, NMe_3), 2.97−2.99 (m, 6H, CH_2).

[{Hg(Tab)$_2$}$_2$(μ-Oxa)](PF$_6$)$_2$·2H$_2$O (8·2H$_2$O). Compound **8**·$2H_2O$ was prepared as colorless blocks in a manner similar to that described for the preparation of **2**, using **1** (0.825 g, 1 mmol) in 15 mL of MeCN and oxalic acid (0.180 g, 2 mmol) in MeOH (3 mL) and H_2O (2 mL). Yield: 0.65 g (89% based on Hg). Anal. Calcd. for $C_{38}H_{56}F_{12}Hg_2N_4O_4P_2S_4$: C, 31.43; H, 3.89; N, 3.86. Found: C, 31.71; H, 3.77; N, 3.99. IR (KBr disk): 3430 (m), 3045 (w), 1604 (s), 1489 (s), 1413 (w), 1312 (w), 1234 (w), 1127 (m), 1010 (w), 957 (w), 846 (s), 746 (w), 559 (m) cm^{-1}. UV−vis (MeCN, λ_{max}(nm (ε M^{-1} cm^{-1}))): 258 (90500). ^1H NMR (400 MHz, $(CD_3)_2SO$): δ 7.58−7.72 (m, 8H, Ph), 3.53 (s, 18H, NMe_3).

[{Hg(Tab)$_2$}$_2$(μ-Adi)](PF$_6$)$_2$ (9). Compound **9** was prepared as colorless blocks in a manner similar to that described for the preparation of **2**, using **1** (0.825 g, 1 mmol) in 15 mL of MeCN and adipic acid (0.146 g, 1 mmol) in H_2O (3 mL). Yield: 0.61 g (81% based on Hg). Anal. Calcd. for $C_{42}H_{60}F_{12}Hg_2N_4O_4P_2S_4$: C, 33.53; H, 4.02; N, 3.72. Found: C, 30.42; H, 3.73; N, 3.89. IR (KBr disk): 3441 (m), 3095 (w), 3045 (w), 2966 (w), 1655 (s), 1585 (m), 1490 (s), 1404 (w), 1313 (w), 1280 (w), 1232 (w), 1127 (m), 1009 (w), 958 (w), 845 (s), 746 (w), 711 (w), 558 (s) cm^{-1}. UV−vis (MeCN, λ_{max}(nm (ε M^{-1} cm^{-1}))): 265 (114000). ^1H NMR (400 MHz, $(CD_3)_2SO$): δ 7.56−7.70 (m, 8H, Ph), 3.54 (s, 18H, NMe_3), 1.94 (m, 2H, CH_2), 1.43 (m, 4H, CH_2).

[Hg(μ-Tab)(μ-Adi)]$_{2n}$ (10). Compound **10** was prepared as colorless blocks in a manner similar to that described for the preparation of **2**, using **1** (0.825 g, 1 mmol) in 15 mL of MeCN and adipic acid (0.292 g, 2 mmol) in H_2O (3 mL). Yield: 0.75 g (75% based on Hg). Anal. Calcd. for $C_{30}H_{42}Hg_2N_2O_8S_2$: C, 35.19; H, 4.13; N, 2.74. Found: C, 35.40; H, 3.87; N, 2.98. IR (KBr disk): 3418 (m), 3057 (w), 2947 (w), 2933 (w), 2909 (w), 2860 (w), 1567 (s), 1487 (s), 1457 (w), 1390 (s), 1314 (m), 1294 (m), 1263 (w), 1125 (w), 1013 (w), 959 (w), 847 (w), 747 (w), 555 (w) cm^{-1}. UV−vis (MeCN, λ_{max}(nm (ε M^{-1} cm^{-1}))): 268 (102000). ^1H NMR (400 MHz, $(CD_3)_2SO$): δ 7.58−7.72 (m, 4H, Ph), 3.54 (s, 9H, NMe_3), 1.90 (m, 2H, CH_2), 1.50−1.52 (m, 4H, CH_2).

[Hg(Tab)$_2$(Meida)]·2.5H$_2$O (11·2.5H$_2$O). Compound **11**·$2.5H_2O$ was prepared as colorless blocks in a manner similar to that described for the preparation of **2**, using **1** (0.825 g, 1 mmol) in 15 mL of MeCN and methylimindiacetic acid (0.292 g, 2 mmol) in H_2O (3 mL). Yield: 0.52 g (72% based on Hg). Anal. Calcd. for $C_{23}H_{38}HgN_3O_{6.5}S_2$: C, 38.09; H, 5.29; N, 5.80. Found: C, 38.31; H, 5.40; N, 5.98. IR (KBr disk): 3389 (s), 3031 (m), 2961 (m), 2913 (m), 1589 (s), 1489 (s), 1403 (s), 1308 (s), 1252 (w), 1128 (w), 1098 (m), 1035 (w), 1010 (m), 958 (m), 888 (m), 848 (m), 823 (m), 746 (m), 546 (m) cm^{-1}. UV−vis (MeCN, λ_{max}(nm (ε M^{-1} cm^{-1}))): 290 (76500). ^1H NMR (400 MHz, D_2O): δ 7.448−7.453 (m, 8H, Ph), 3.48 (s, 18H, NMe_3), 2.94 (m, 4H, CH_2), 2.16 (s, 3H, Me in Meida).

X-ray Structure Determinations. Single crystals of **2**·$0.5H_2O$, **3**, **4**·MeOH, **5**·MeOH, **6**·H_2O, **7**·H_2O, **8**·$2H_2O$, **9**, **10**, and **11**·$2.5H_2O$ suitable for X-ray analysis were obtained directly from the above preparations. All measurements were made on a Rigaku Mercury CCD X-ray diffractometer by using graphite monochromated Mo Kα (λ = 0.71073 Å) radiation. Each single crystal was mounted at the top of a glass fiber, and cooled at 193 K for **2**·$0.5H_2O$, **3**, **4**·MeOH, **6**·H_2O, **7**·H_2O, **8**·$2H_2O$, **9**, **10**, and **11**·$2.5H_2O$, 213 K for **5**·MeOH in a stream of gaseous nitrogen. Diffraction data were collected at ω mode with a detector-to-crystal distance of 35 mm. Cell parameters were refined by using the program Crystalclear (Rigaku and MSc, Ver. 1.3, 2001) on all observed reflections. The collected data were reduced by using the program CrystalClear (Rigaku and MSc, Ver. 1.3, 2001), and an absorption correction (multiscan) was applied. The reflection data were also corrected for Lorentz and polarization effects.

The crystal structures of **2**·$0.5H_2O$, **3**, **4**·MeOH, **5**·MeOH, **6**·H_2O, **7**·H_2O, **8**·$2H_2O$, **9**, **10**, and **11**·$2.5H_2O$ were solved by direct methods and refined on F^2 by full-matrix least-squares using anisotropic displacement parameters for all non-hydrogen atoms.[37] The H_2O molecule in **2**·$0.5H_2O$ was found to be disordered over two positions with an occupancy factor of 0.598/0.402 for O(1)/O(1A). The hydrogen atoms of the H_2O and MeOH solvent molecules in **2**·$0.5H_2O$, **4**·MeOH, **5**·MeOH, **6**·H_2O, **7**·H_2O, **8**·$2H_2O$, and **11**·$2.5H_2O$ were located from Fourier maps and their O−H bond distances were restrained to be equal to 0.85. All other hydrogen atoms were placed in geometrically idealized positions (C−H = 0.98 Å for methyl groups; C−H = 0.95 Å for phenyl groups) and constrained to ride on their parent atoms with $U_{iso}(H) = 1.5U_{eq}(C)$ for methyl groups and $U_{iso}(H) = 1.2U_{eq}(C)$ for phenyl groups. Important crystal data and collection and refinement parameters for **2**·$0.5H_2O$, **3**, **4**·MeOH, **5**·MeOH, **6**·H_2O, **7**·H_2O, **8**·$2H_2O$, **9**, **10**, and **11**·$2.5H_2O$ are given in Table 4.

Acknowledgment. This work was financially supported by the National Natural Science Foundation of China (20525101, 20871088, and 90922018), the Nature Science Key Basic Research of Jiangsu Province for Higher Education (09KJA150002), the Specialized Research Fund for the Doctoral Program of higher Education of Ministry of Education (20093201110017), the State Key Laboratory of Coordination Chemistry of Nanjing University, the Qin-Lan and the "333" Projects of Jiangsu Province, and the "Soochow Scholar" Program and the Program for Innovative Research Team of Suzhou University. The authors also highly

(36) (a) Hasnain, S. S. In *Synchrotron Radiation in Chemistry and Biology II*; Mandelkow, E., Ed.; Springer-Verlag: New York, 1988; p 73. (b) Eichhofer, A.; Buth, G. *Eur. J. Inorg. Chem.* **2005**, 4160.

(37) Sheldrick, G. M. *SHELXS-97 and SHELXL-97, Program for the X-ray Crystal Structure Solution*; University of Göttingen: Göttingen, Germany, 1997.

appreciated the helpful comments from the editor and the reviewers.

Supporting Information Available: Crystallographic data of **2**·0.5H_2O, **3**, **4**·MeOH, **5**·MeOH, **6**·H_2O, **7**·H_2O, **8**·2H_2O, **9**, **10**, and **11**·2.5H_2O (CIF), and views of the hydrogen-bonded networks for **2**·0.5H_2O, **3**, **4**·MeOH, **5**·MeOH, **6**·H_2O, **7** H_2O, **8**·2H_2O, **9**, **10**, and **11**·2.5H_2O in PDF format. This material is available free of charge via the Internet at http://pubs.acs.org.